The expression levels of Toll-like receptors after metal particle and ion stimulation in the synovium *in vivo*.

Xiangyun Cheng

München 2022

Aus der Klinik für Orthopädie und Unfallchirurgie
der Universität München

vormals Klinik und Poliklinik für Orthopädie, physikalische Medizin und Rehabilitation

Direktor: Prof. Dr. med. Boris Holzapfel
Prof. Dr. med. Wolfgang Böcker

The expression levels of Toll-like receptors after metal particle and ion stimulation in the synovium *in vivo*

Dissertation
zum Erwerb des Doktorgrades der Humanbiologie
an der Medizinischen Fakultät der
Ludwig-Maximilians-Universität zu München

vorgelegt von

Xiangyun Cheng

aus

Jining, China

2022

Mit Genehmigung der Medizinischen Fakultät
der Universität München

Berichterstatter:	PD Dr. Alexander C. Paulus
Mitberichterstatter:	Prof. Dr. Christian Zeckey
	PD Dr. Oliver Pieske
Mitbetreuung durch den promovierten Mitarbeiter:	----------
Dekan:	Prof. Dr. med. Thomas Gudermann
Tag der mündlichen Prüfung:	05.04.2022

Eidesstattliche Erklärung

Ich erkläre hiermit an Eidesstatt,

dass ich die vorliegende Dissertation mit dem Titel „The expression levels of Toll-like receptors after metal particle and ion stimulation in the synovium *in vivo*." selbständig verfasst, mich außer der angegebenen keiner weiteren Hilfsmittel bedient und alle Erkenntnisse, die auf dem Schrifttum ganz oder annähernd übernommen sind als solche kenntlich gemacht und nach ihre Herkunft unter Bezeichnung der Fundstellen einzeln nachgewiesen habe.

Ich erkläre des Weiteren, dass die hier vorgelegte Dissertation nicht in gleicher oder in ähnlicher Form bei einer anderen Stelle zur Erlangung eines akademischen Grades eingereicht wurde.

Beijing, am 03.04.2022 Xiangyun Cheng

To my family

Table of Contents

Zusammenfassung

HINTERGRUND: Die aseptische Protheselockerung spielt nach wie vor eine relevante Rolle in der Endoprothetik und verursacht einen Großteil der notwendigen Revisionsoperationen. Im Synovialgewebe um ein Implantat tritt eine aseptische inflammatorische Reaktion auf, die durch solide Verschleißpartikel und ggf. durch Metallionen verursacht wird. Über eine komplexe Kaskade kommt es letzten Endes zu einer osteolytischen Reaktion rund um die einliegende Endoprothese. Dies wird als Hauptfaktor für die Lockerung des sterilen Implantats angesehen. Obwohl der Mechanismus der aseptischen proinflammatorischen Reaktion auf Verschleißpartikel und Metallionen noch nicht vollständig geklärt ist, haben viele Arbeitsgruppen darauf hingewiesen, dass solide Verschleißpartikel, aber auch eben Metallionen durch Aktivierung verschiedener Toll-like Rezeptoren (TLR) aseptische proinflammatorische Reaktionen auslösen können. Bisher wurde jedoch die genaue Rolle verschiedener TLRs bei der Regulierung der aseptischen proinflammatorischen Reaktion von Verschleißpartikeln und Metallionen noch nicht eingehend untersucht. In Anbetracht der obigen Situation besteht der Zweck dieser Studie darin, die Zelloberflächenrezeptoren (spezifische TLRs) zu bestimmen, die eine signifikante Reaktion auf die Stimulation von Verschleißpartikeln und Metallionen in einem etablierten in-vivo-Modell haben. Ferner sollte ein reaktiver Unterschied von soliden Abriebpartikeln und Ionen in der Synovialmembran bei der Aktivierung von TLRs herausgearbeitet werden.

METHODEN: In dieser Studie wurde die in orthopädischen Implantaten übliche Standardlegierung aus Kobalt-Chrom-Molybdän (CoCrMo) (ISO 5832-12 / ASTM F1537) ausgewählt, um CoCrMo-Partikel (CP) und CoCrMo-Ionen (CI) herzustellen. Es wurden 30 weibliche Balb / c-Mäuse zufällig in drei Gruppen á 10 Tieren eingeteilt, und so Gruppe CP CoCrMo-Partikel, Gruppe CI CoCrMo-Ionen und Gruppe PBS phosphatgepufferte Salzlösung (PBS, Kontrolle) in das murine linke Kniegelenk injiziert. Sieben Tage nach der Injektion wurden die Tiere euthanasiert, es folgte die immunhistochemische Analyse in der Synovialschicht der murinen Kniegelenke unter Verwendung der polyklonalen TLRs 1, 2, 4, 5 und 6.

ERGEBNISSE: Neben einer verdickten Synovialmembran und einer intensiven Infiltration entzündlicher Zellen zeigte die mit CoCrMo-Partikeln injizierte Gruppe im Vergleich zur PBS-Gruppe eine signifikant hochregulierte TLR-Expression (TLRs 1, 2, 4, 5 und 6). Die CP-Gruppe hatte auch eine höhere Expression der TLRs 1, 4 und 6 als die CI-Gruppe ($p < 0,0167$). Interessanterweise gab es auch sichtbare Korrosionspartikel im nekrotischen Gewebe der CP-Gruppe. Die Expressionsniveaus von TLR4 und TLR6 in der CI-Gruppe waren signifikant höher als die in der PBS-Gruppe ($p < 0,0167$).

SCHLUSSFOLGERUNGEN: Die Ergebnisse dieser Untersuchung legen nahe, dass CoCrMo-Partikel zu einer robusten proinflammatorischen Reaktion und einer erhöhten Expression von Zelloberflächen-TLRs führen. Darüber hinaus weisen die grünen

Korrosionspartikel in dieser Studie darauf hin, dass CoCrMo-Partikel ein bestimmtes Maß an lokalen toxischen Metallionen in der Synovialschicht des Kniegelenks freisetzen können. Nach der Implantation von CoCrMo-Ionen in das Kniegelenk des Mausmodells sind die Spiegel von TLR 4 und 6 sehr hoch. Die aktuellen Ergebnisse zeigen, dass es einen signifikanten Unterschied in der Expression von TLRs zwischen den in dieser Studie verwendeten CoCrMo-Partikeln und CoCrMo-Ionen gibt.

Summary

OBJECTIVE: Aseptic loosening is still one of the most challenging long-term complications in modern arthroplasty and contributes significantly to growing numbers of necessary revision arthroplasty. The sterile inflammatory response to wear particles and ionic products within the peri-implant synovial-like tissue is regarded as a central factor contributing to aseptic implant loosening. Although the mechanisms of the sterile inflammatory response to wear particles and ionic products are still not fully understood in detail, many researchers indicate that these by-products released from implants may trigger the sterile pro-inflammatory response by activating distinct Toll-like receptors (TLRs). However, to date, the exact roles of distinct TLRs in regulating the sterile pro-inflammatory response to wear particles and ionic products have not been fully clarified. In light of the situation described above, this investigation aimed to determine the potential cell surface receptors (specific TLRs) activated in response to wear debris particles and ionic products, and to evaluate the difference in TLR expression levels between wear particles and ionic products in the knee joint synovial tissues of a murine model.

METHODS: Standard cobalt-chromium-molybdenum alloys (CoCrMo) that are commonly used in orthopedic implants were chosen to harvest CoCrMo wear particles (CP) and CoCrMo ionic products (CI) in this investigation. Thirty female Balb/c mice that were randomly assigned to three groups (each sized 10 animals) received intra-articular injections of CoCrMo particles (CP group), CoCrMo ions (CI group), or PBS

solution (phosphate-buffered saline; the control group). When the injection was finished, all groups would continue to be fed for seven days. Subsequently, anti-TLR 1, 2, 4, 5, and 6 antibodies were used to do immunohistochemical analysis within the murine knee joint synovial tissues.

RESULTS: In addition to a thickened synovial membrane and intense inflammatory cell infiltrates, the group injected with CoCrMo particles showed significantly upregulated TLR expression (TLRs 1, 2, 4, 5, and 6) compared with the PBS group and higher expression of TLRs 1, 4, and 6 than the CI group ($p < 0.0167$). Interestingly, greenish corrosion particles were also observed in the necrotic tissue of the CP group. Additionally, significantly higher levels of TLRs 4 and 6 in the CI group were found than those in the PBS group ($p < 0.0167$).

CONCLUSIONS: This investigation suggests that CoCrMo particles lead to an intense pro-inflammatory reaction and elevated expression of cell surface TLRs. Moreover, the greenish corrosion particles observed in this investigation show that CoCrMo particles might release a certain level of locally toxic metal ions in the murine knee joint synovial tissues. After the murine model receive the intra-articular injection of CoCrMo ionic products, significantly higher levels of TLRs 4 and 6 are observed than those in the PBS group. The current results expose obvious differences in TLR expression induced by CoCrMo particles and ionic products used in this investigation *in vivo*.

1. Introduction

Although the biological mechanisms of aseptic implant loosening have not yet been comprehensively elucidated, biological responses to wear debris particles and metallic ionic products around arthroplasty implants are tightly associated with aseptic implant loosening [1]. This introduction reviews and summarizes the current status of the research involving aseptic implant loosening according to the relevant literature. Meanwhile, the roles of cell surface Toll-like receptors in triggering sterile inflammatory reactions in peri-prosthetic tissues are briefly introduced to outline the theoretical basis of this investigation.

1.1 Aseptic implant loosening

Total hip replacement [2] is regarded as one of the most efficacious and common surgeries for treating severe posttraumatic, degenerative, and other diseases of the hip joint [3]. Because of the excellent postoperative results and the patients' high satisfaction, THRs have been designated "the operation of the century [4]". More than one million THRs are estimated to be performed annually worldwide [5]; moreover, according to some modeled future projections, the need for THRs is expected to increase further in the future [6]. However, prosthetic implants cannot be normally utilized in the human body forever. Commonly, after 15 to 20 years, more than 10% of patients who receive primary THR must undergo revision surgery, which usually has a longer and more complex surgical procedure and a poorer postoperative outcome than primary surgery [7]. Due to improvements in implant materials, operative procedures,

patient selection, and pain control, revision surgeries caused by dislocations, fractures, and sepsis have become relatively rare, whereas revision surgeries caused by aseptic implant loosening are becoming much more prominent, even accounting for approximately 70% of the overall revision surgeries [8-11]. Considering this situation, studies examining the pathophysiology of aseptic implant loosening are critical and well justified, not only for prevention but also for further treatment [12].

Aseptic implant loosening refers to the loosening of an implant from the bone bed without the presence of pathogen interference or trauma [5, 13] (**Figure 1**). Generally, aseptic implant loosening is accompanied by loss of function and pain, while it sometimes also occurs asymptomatically [14, 15]. Concerning the prevention of aseptic loosening, the critical point is to determine what mechanism initially destroys the stable bond between the bone bed and the implant [5, 16]. A sole mechanical theory was once proposed. Supporters of the mechanical theory indicated that mechanical stress and strain are the critical drivers of aseptic implant loosening [17]. They postulated that stress and strain affect the implant-bone interface during each movement of patients until they devastate the firm bond between the bone bed and the implant [17, 18]. In this theory, the importance of initial firm fixation and accurate implant placement are stressed.

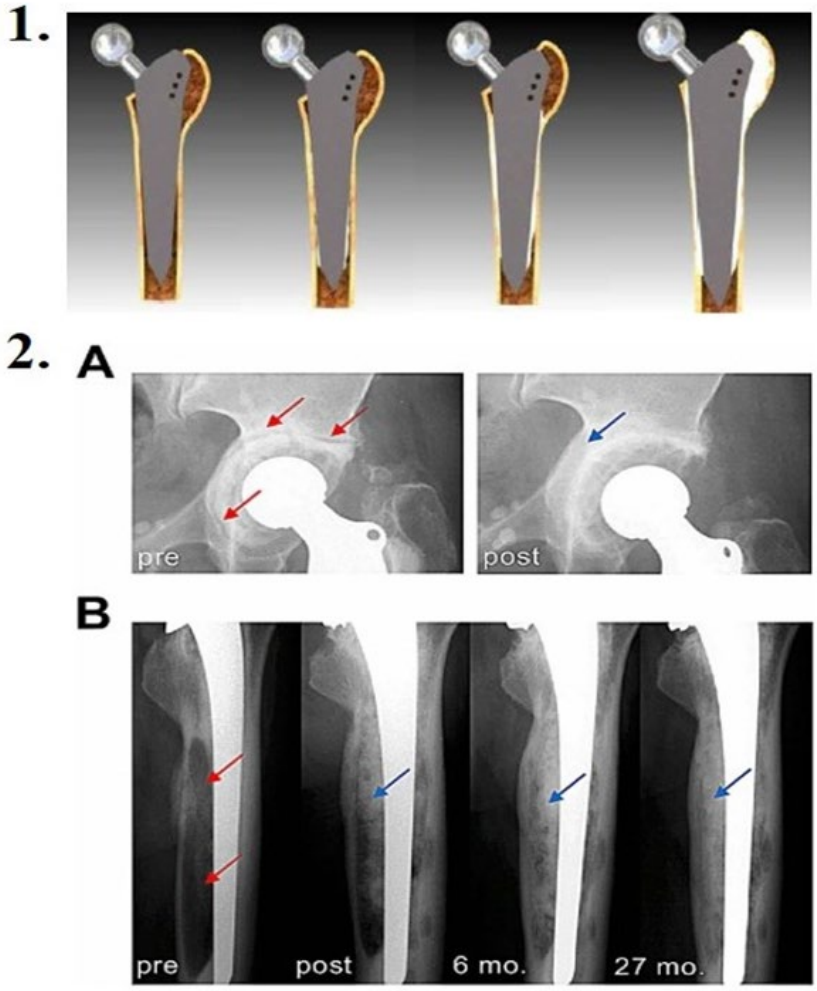

Figure 1. Aseptic implant loosening around hip implants. 1. The process of gradual stem loosening. During the process of aseptic implant loosening, the synovial-like membrane (white) is gradually thickened. 2. Radiographic images of aseptic implant loosening (red arrow) and new radiographic images after revision surgery (blue arrow). Red arrows showed the circumferential signs of loosening. Blue arrows showed the increasing bony consolidation after revision hip replacement. (1. Taken from Gallo et al. 2012 [5]; 2. Taken from Rolvien et al. 2020 [18].)

Meanwhile, some supporters have indicated that early migration of the prosthesis is tightly associated with the premature failure of THRs [19, 20]. Regrettably, a consensus threshold of migration to predict aseptic implant loosening has not been established [21]. Moreover, most cemented cups usually migrate in the first year without loss of

function after THRs [22]. Thus, the prediction of patients who need revision surgeries by assessing the migration of the prosthesis is difficult. Therefore, the sole mechanical theory does not explain many issues. In addition to the sole mechanical theory, a biological theory was also proposed. In 1977, Willert et al. [23] initially proposed that periprosthetic biological reactions to wear debris released from the implant were the leading cause of aseptic implant loosening. Different levels of wear particles and metallic ions are unavoidably released from wear or electrochemical corrosion between the implant-bone interfaces, articulating surfaces, or between modular interfaces of THRs [24, 25]. Various periprosthetic cells are stimulated after large amounts of wear debris particles and metallic ionic products are released from implants [24]. Subsequently, pro-inflammatory/pro-osteoclastic cytokines and other biomolecules might be secreted and lead to osteoclast accumulation [13]. Osteolysis and aseptic loosening will eventually occur in response to the chronic long-term stimulation of wear particles and metallic ions [26, 27]. Commonly, many wear particles, macrophages, lymphocytes, giant cells, histiocytes, fibroblasts, neutrophils, and plasma cells are observed in the tissues retrieved from around implants during revision surgeries, indicating that biological reactions to wear debris are in progress [6].

Based on these discoveries, researchers currently estimate that both mechanical and biological events might not be underestimated [28, 29]. Biological reactions to wear debris are relevant to aseptic loosening [30]. However, stress shielding, joint fluid pressure and flow, aging of the bone bed, and mechanical wear also undoubtedly

contribute to the loss of implant-bone fixation [10, 31, 32]. Therefore, great efforts are ongoing to design more wear-resistant materials [33]. Additionally, because the problem of premature loosening of the prosthesis remains and the complexity of biological reactions has not yet been fully clarified, efforts to elucidate biological responses to wear debris are equally critical.

1.2 Biological reactions in the periprosthetic tissue

Biological responses in periprosthetic soft and bone tissues, also designated adverse local tissue reactions (ALTRs), are mainly initiated by wear particles, metal oxides, and free metallic ions [34, 35]. According to the literature, ALTRs include inflammation; ischemia; osteoclast-, osteoblast-, fibroblast-driven reactions; and even hypersensitive responses [29, 36, 37]. Typical findings resulting from ALTRs in total hip arthroplasties are briefly introduced below.

Synovial-like interface membrane (SLIM) between the bone and implant/cement is a common histological finding [38, 39]. Initially, in radiographic testing, an important feature of aseptic loosening is the presence of a radiolucent line at the bone-implant interface that indicates a peri-implant bone loss or fixation failure [18, 40]. Coincidentally, SLIMs are invariably found at the bone-implant interface in revision surgeries [41]. Thus, the synovial-like interface membrane is suspected to be associated with the peri-implant bone loss [42, 43]. Based on several histopathological studies, SLIMs predominantly contain scattered wear particles, macrophages, fibroblasts, giant

cells, endothelial cells, and other components, showing remarkable similarities to the rheumatoid synovium [44, 45]. In addition, high expression of proinflammatory cytokines and other mediators have also been detected in SLIM samples [24]. Commonly, macrophages, fibroblasts, and high levels of pro-inflammatory mediators are very important factors typical of chronic inflammation, which can gradually result in the formation of chronic fibrosis and osteolysis around the prosthesis [46, 47]. As outlined above, SLIMs are highly relevant to aseptic implant loosening and have attracted increasing attention from scientific communities.

According to the Anglo-American literature, the standard term "synovial-like interface membrane" (SLIM) is usually used to refer to the periprosthetic membrane, pseudomembrane, and regenerated synovial tissue [38]. However, in certain situations, especially when periprosthetic tissues display severe foreign body-type reactions to wear particles, some researchers also use the term "granulomatous tissue" to describe periprosthetic tissues [12, 48, 49]. In this context, granuloma (pseudotumor) is observed in the SLIM, representing neosynovial aggressive growth with or without tissue necrosis [50-52]. The general mechanisms underlying granuloma (pseudotumor) formation are described briefly. The slow release of wear particles activates macrophages to phagocytize many toxic particles, which results in cell death by cytotoxicity, necrosis, or apoptosis [51, 53]. These wear particles remain in the tissue, resulting in new monocyte/macrophage recruitment, cytotoxicity, and chronic pro-inflammatory reactions [54]. Thus, a stressful environment is established around the

prosthesis that may induce chronic necrosis, fibrosis, the formation of granuloma (pseudotumor), and ultimately, osteolysis (**Figure 2**) [51, 54, 55].

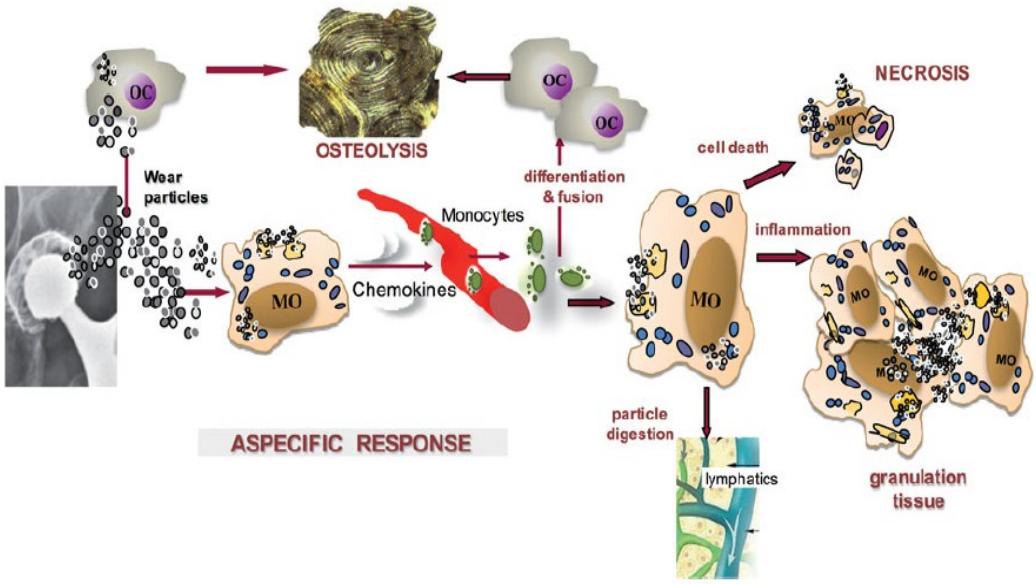

Figure 2. Biological reactions caused by wear debris around hip implants. Wear debris is released to the implant-bone interface. The wear debris will be phagocytized by macrophages (MO) within the synovial-like tissue. And some wear debris may be phagocytized by osteoclasts (OC). After the phagocytosis, macrophages will release pro-inflammatory mediators which can recruit more monocytes/macrophages. Additionally, some wear debris may be disseminated to remote tissue by lymphatic vessels and blood vessels. Excessive particle discharge may lead to cell death, and tissue necrosis, finally end with granulomatous tissue formation. (Taken from Granchi et al. 2018 [51])

In addition to cytotoxic reactions, type IV hypersensitivity reactions to metallic particles and metallic ions have also been mentioned as one of the mechanisms underlying granuloma (pseudotumor) formation in several studies [51, 56]. The consideration of type IV hypersensitivity reaction is principally due to the large number of T-lymphocytes in peri-implant tissues (granulomas) and to the capability of metallic ionic products to trigger allergic reactions by acting as haptens [57-59]. However, unlike sterile inflammation, researchers have not yet determined whether and the extent

to which classical allergic reactions to metallic particles and ionic products contribute to aseptic osteolysis [49]. Solid opposition to the hypersensitivity theory was reported previously. Concerning type IV hypersensitivity reactions, about ten percent of the populace is allergic to the metallic alloys in costume jewelry, coins, and joint arthroplasties [27]. Suppose that metallic particles and ions cause severe contact allergies. In that case, usually small amounts of allergens induce very strong hypersensitive (allergic) reactions; thus, many more revision arthroplasties should have been conducted due to "allergic issues", which have not really occurred [49].

Additionally, in a study using a murine model, significantly increased pro-inflammatory cytokine expression and macrophage infiltration were observed in the thickened synovial layer after metallic debris stimulation. However, CD 3-positive cells (T-lymphocytes) did not show a significantly augmented number than those in the control group [24]. Therefore, in the current situation, avoiding inflammatory reactions around the prosthesis, but not type IV hypersensitivity reactions, appears to be more critical. Additionally, in terms of patients who are allergic to metals, prudence and caution are needed when deciding their treatment procedures because we should avoid the potential adaptive immune responses [60] (**Figure 3**).

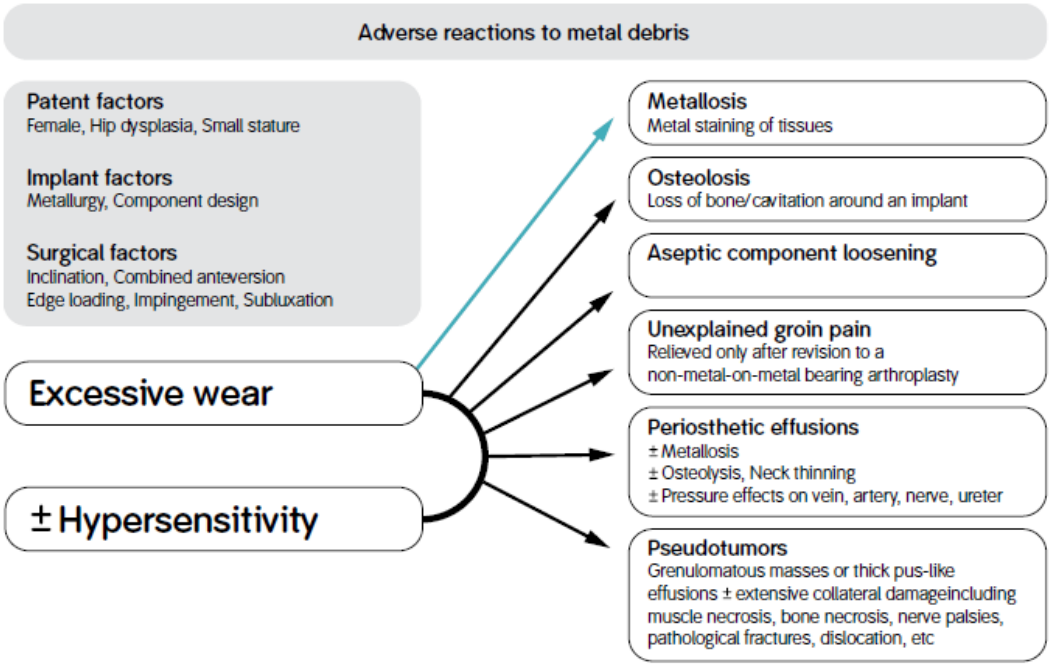

Figure 3. The summary of local adverse reactions to metal debris. (Taken from Quigley et al. 2010 [60])

1.3 Wear and corrosion of orthopedic prosthesis materials

This section is mainly focused on the wear and corrosion of cobalt-chromium-molybdenum (CoCrMo) metallic alloys. When applied in the metal-on-metal (MoM) [61] prosthetic joint, these CoCrMo metals release large amounts of particles and ions, which have been found to cause adverse local tissue reactions and even systemic events [62, 63]. Modern CoCrMo alloys are principally categorized by the American Society for Testing and Materials (ASTM) [64] or International Organization for Standardization (ISO) and are divided into two groups: cast alloys (ASTM F75, ISO 5832-4) and wrought alloys (ASTM F1537, ISO 5832-12) [65-67]. Cast CoCrMo alloys have been used in dentistry for several years and afterward in orthopedic implants [68]. These cast alloys are usually used to produce complex shapes that cannot be machined,

e.g., the acetabular cup of THRs [67, 69]. Wrought CoCrMo alloys usually have homogeneous microstructures and superior mechanical and fatigue properties [70]. Therefore, wrought CoCrMo alloys can also be used to generate modular femoral heads and hip stems [71].

CoCrMo alloys were initially introduced as one replacement for gold in dentistry at the beginning of the 1930s [72]. Later, with the improvement of their bulk mechanical properties via several advanced material processing techniques, CoCrMo alloys have been approved for use as the only materials of MoM articulations since the early 1970s [70]. Subsequently, due to the excellent clinical performance of metal-on-polyethylene (MoP) implants reported during the 1970s and 1980s, the use of MoM articulations composed of CoCrMo alloys subsequently decreased momentously [72, 73]. However, afterward, MoP implants were shown to have a higher volumetric wear rate than MoM articulations, and polyethylene particles were also observed in periprosthetic tissues [74]. Thus, in the early 1990s, second-generation MoM articulations were recommended and attracted renewed interest because of their high corrosion resistance and low volumetric wear rate [69, 75]. According to the literature, the volumetric wear rate in MoM couples after the running-in stage is approximately 0.3 μm^3/year, which is approximately 100 times lower than that in MoP articulations [76]. However, in the later 2000s, national joint registries reported the failure rate of THRs with MoM articulations to be 2-3 times higher than that of modern THRs without MoM articulations [77]. Meanwhile, metallic particles and ions were regarded as a significant

cause of failure in patients with MoM implants [77]. Therefore, a clearer comprehending of the physical and chemical properties of metallic particles and ions is needed.

1.3.1 CoCrMo particles

CoCrMo particles are released due to wear between articular surfaces, non-articular surfaces, or between modular interfaces of THRs [24, 78]. After these metal particles are released, they are usually scattered in the implant-bone interface; additionally, with synovial fluid involvement, some nanoparticles are probably delivered to the bone, blood vessels, and lymphatics [79]. Then, they are disseminated to other distant organs via blood vessels and lymphatics [24]. Therefore, adverse reactions caused by metal particles possibly occur at new sites in the host body.

Three central mechanisms have been identified to explain the wear of arthroplasty bearing surfaces: adhesive wear, fatigue wear, and abrasive wear [51, 80]. Adhesive wear involves the intermolecular bonds of two different materials resulting in more significant shearing. Cyclic stresses cause fatigue wear of the implants during friction. Abrasive wear occurs when hard materials slide across soft materials, such as bone fragments or bone cement between two articular surfaces [51].

Wear particles used for studies are mainly generated from three sources, including revision surgeries, joint simulators, and sliding-wear tribometers [81-83]. Although

wear particles obtained from revision surgeries are very helpful to understand the general wear mechanisms and adverse reactions, they are challenging to attain because of the limited number of patients undergoing revision surgeries [24]. Wear particles obtained from simulator tests and tribometer tests provide further insights into the wear of joint implants [84, 85]. Additionally, a sufficient number of samples from simulator tests and tribometer tests can be used to study biological reactions to wear particles *in vivo* and *in vitro*.

Commonly, the biological response caused by wear debris is related to the particle number, size, volume, type, composition, and chemical properties [12, 86]. Although the size of released particles varies, most CoCrMo particles are usually less than 100 nm in size [87], which is smaller than polyethylene debris (0.1-2 μm) [88]. As described above, the volumetric wear rate in MoP articulations is approximately 100 times higher than that in MoM couples [76]. However, the total amount of CoCrMo debris generated in MoM implants is approximately 13-500 times greater than that in MoP implants [76]. Thus, compared with MoP implants, MoM implants release more metal particles at the same volume.

Additionally, the majority of CoCrMo particles are round and oval in shape, while a variable number presents an elongated or needle-like shape [11, 79]. Generally, the chemical composition of CoCrMo particles measured utilizing energy-dispersive X-ray spectroscopy (EDS) is comparable to that of original CoCrMo metallic alloys, which is

mainly a combination of Cr, Mo, and Co elements [89]. However, some particular debris isolated from CoCrMo implants was also observed, such as some amorphous metal particles containing only O and Cr with little to no Mo and Co [79, 90]. Many physical and chemical alterations of metal particles remain unknown and require further investigation.

1.3.2 CoCrMo ions

During the manufacturing process, a dense protective oxide membrane will be formed on the outer layer of CoCrMo implants [87]. The protective oxide membrane is detected to be 1-4 nm thick and avoids severe corrosion reactions by blocking the contact between the metal and the solution [91]. However, after implantation, the very thin oxide film is prone to fracture because of wear and mechanical loading, resulting in exposure of the reactive base element to the physiological environment in the human body [92].

In general, cobalt and chromium are reactive in water solution, even under conditions lacking applied potentials [87]. Re-passivation and dissolution reactions relevant to metallic oxide formation and metallic ion generation will occur in the human body after the thin oxide layer is damaged. Occasionally, molybdenum is also involved in related reactions [87, 92]. The main reactions are as follows [92].

Oxide passivation reactions: $H_2O + Co \rightarrow 2H^+ + CoO + 2e^-$

$$2Cr + 3H_2O \rightarrow 6H^+ + Cr_2O_3 + 6e^-$$

$$3Mo + 3H_2O \rightarrow 3MoO + 6H^+ + 6e^-$$

Dissolution reactions: $Co \rightarrow Co^{2+} + 2e^-$

$$Cr \rightarrow Cr^{3+} + 3e^-$$

$$Mo \rightarrow Mo^{2+} + 2e^-$$

With the progress of these reactions, a certain amount of metallic ions will be released into the synovial fluid of the joints [92]. In addition to metal implants, the passivation and dissolution reactions of wear particles cannot be neglected. Most of the CoCrMo particles released from the metal implant are usually less than 100 nm in size. A smaller size will allow a certain volume of particles to have a larger contact area with the physiological environment. Additionally, nanoparticles (30-60 nm) can be directly phagocytized by macrophages [93]. Commonly, macrophages are known to create an acidic environment by generating hydrochloric acid (HCl) [94, 95]. The pH value of lysosomes used to digest foreign bodies in macrophages ranged from 3.5 to 5.5, which obviously affects the corrosion rate of CoCrMo particles [96-98]. A more acidic environment results in a higher corrosion rate of CoCrMo particles [92]. In addition to the acidic environment, several reactive oxygen species can be generated by numerous macrophages, including superoxide, hydroxyl radicals, sodium hypochlorite (HClO), and hydrogen peroxide [92, 99]. Electrochemical reactions occur between the CoCrMo

particles and these reactive oxygen species. Subsequently, more metal ions will be generated via these redox reactions.

Possible electrochemical reactions involving reactive oxygen species are shown as below:

$5H_2O + Cr_2O_3 \rightarrow 8H^+ + 2HCrO^{4-} + 6e^-$ (pH < 6. 5)

$2H^+ + CoO \rightarrow H2O + Co^{3+} + e^-$ (pH < 8)

$H_2O_2 + P^{n+} \rightarrow OH + M^{(n+1)+} + OH^-$ (P: Co; Cr; Mo)

$3ClO^- + 2Cr^{3+} + 3H_2O \rightarrow +3Cl^- + 6OH^- + 2Cr^{6+}$

During the process of metal ion generation, nanoparticles probably react with several cellular components such as proteins, reactive oxygen species (ROS), and DNA, extensively changing the biological surroundings and leading to functional and structural damage to cells [100]. The released metal ions are also toxic at high concentrations, which probably results in local sterile inflammation, tissue necrosis, and the death of inflammatory cells [101]. Additionally, metallic ions can be delivered to the bone, lymphatics, and blood vessels via the joint fluid. Subsequently, metallic ions are disseminated to other distant organs through the blood and lymph circulation [102, 103]. It has been widely reported that the concentration of metallic ions is significantly upregulated in the serum/blood after MoM joint replacements. Jacobs et al. [104] observed the cobalt and chromium concentrations in urine and serum from 14

participants with MoM THRs. They found that the concentration of chromium in serum increased three-fold and nine-fold in the short- (within 2 years) and long-term (within 20 years), respectively. The concentration of chromium in urine also increased four times and 35 times in the short- (within 2 years) and long-term (within 20 years), respectively [104].

According to the literature, metallic ions released from prostheses are bound by the proteins in the body and form so-called haptens [105, 106]. These haptens can trigger innate or adaptive immune reactions after recognition by some cell receptors [107]. Therefore, some receptors involved in inflammation and adaptive immune responses are also a focus of studies examining biological reactions to metal debris. Typical cell receptors, Toll-like receptors, will be introduced in the next section.

1.4 Toll-like receptors

Pattern recognition receptors (PRRs) are usually regarded as triggers of infectious immune reactions and activate pathways that lead to the secretion of numerous pro-inflammatory mediators [108]. However, periprosthetic sterile inflammatory reactions are also currently considered mediated by some PRRs [109]. Toll-like receptors (TLRs), one type of typical PRRs, not only identify danger- and pathogen-associated molecular patterns (DAMPs and PAMPs) but also transduce signals that lead to the secretion of some inflammatory mediators, such as IL-1β, IL-6 and TNF-α [110]. Additionally, high expression levels of specific TLRs were observed in periprosthetic tissues retrieved

from revision surgeries [111-113]. Hence, TLRs have been focused on in some studies of aseptic implant loosening [114]. Researchers have indicated that wear debris released from implants could directly or indirectly activate specific TLRs. After activation, these receptors (TLRs) transduce danger signals, resulting in the up-regulation of pro-inflammatory mediators **(Figure 4**) [115].

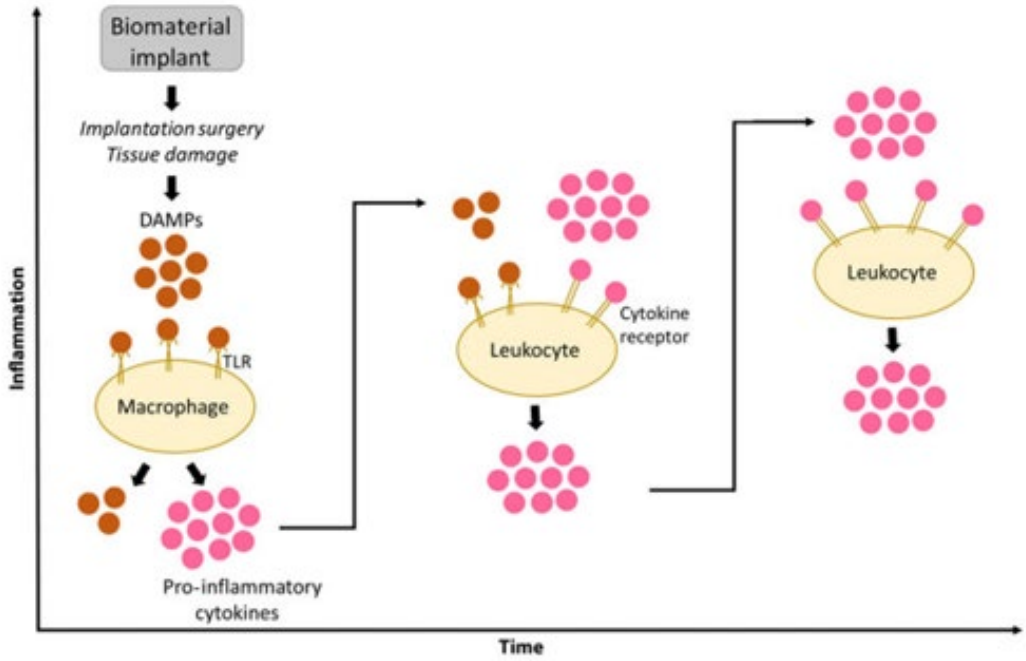

Figure 4. Biomaterials induce inflammatory responses by interacting with TLRs. Macrophages and other white blood cells have critical effects on inflammation. After TLRs are activated on these cells, more pro-inflammatory cytokines and chemokines will be released. (Taken from McKiel et al. 2020 [115])

Thus far, there are thirteen different mammalian TLRs that have been found by scientific communities [116]. Ten TLRs have been identified in human beings (TLR 1 to TLR 10). Twelve TLRs are expressed in mice (TLRs 1-9, 11, 12, and 13) [117]. TLR 1-9 are present in both humans and mice [117]. With regard to TLRs 1, 2, 4, 5, and 6, these receptors are usually expressed on the cellular surface. Thus, these receptors have

the high possibility of direct interactions with wear debris. Nevertheless, commonly, each TLR binds several different ligands, and are even called promiscuous receptors. Hence, due to the functional diversity of TLRs, the exact role of each TLR involved in periprosthetic inflammation caused by wear debris is still controversial.

1.4.1 TLR 1

TLR 1, also designated CD 281 (cluster of differentiation 281), mediates the production of cytokines necessary to develop effective immunity [118]. According to the literature, TLR 1 has been detected on the cell membrane of fibroblasts, synoviocytes, macrophages, dendritic cells, and lymphocytes [119]. Additionally, the TLR 1 gene is ubiquitous, which usually has a higher expression level than other TLR genes. In infectious inflammation, TLR 1 identifies lipopeptides and peptidoglycan in concert with TLR 2 (as a heterodimer) [120]. Additionally, high expression levels of TLR 1 were reported in the tissue around implants composed of titanium metals [121]. Therefore, TLR 1 might be tightly relevant to the sterile inflammatory response caused by wear debris in peri-implant tissues.

1.4.2 TLR 2

TLR 2, also known as CD 282 (cluster of differentiation 282), was first reported in 1998 [122]. TLR 2 is the only Toll-like receptor described to date to generate functional heterodimers with both TLR 1 and 6. Moreover, TLR 2 recognizes various ligands and transduces pathogen- or damage-associated signals via heterodimerization with TLR 1

or TLR 6 [123]. In the absence of TLR 1 and TLR 6, TLR 2 homodimerization was proposed, but further experiments are required to confirm this hypothesis. Additionally, some new studies also indicate the existence of TLR 2/TLR 10 preformed dimers; however, their function has not yet been clearly determined [123]. TLR 2 is usually present on the cell surface of various inflammatory cells, fibroblasts, and other cell types. Due to the wide range of roles and functions of TLR 2, many studies relevant to aseptic implant loosening have focused on the relationship between wear debris and TLR 2. Using a murine calvarial model that can reflect osteolysis caused by wear debris, Greenfield et al. [124] indicated that TLR $2^{-/-}$ mice presented more limited osteolysis than wild-type mice. Moreover, TLR $2^{-/-}$ macrophages secrete fewer pro-inflammatory mediators than normal macrophages after the titanium particle challenge [124]. Therefore, these *in vitro* and *in vivo* data indicated that TLR 2 might be tightly associated with aseptic implant loosening.

1.4.3 TLR 4

In 1999, Qureshi et al. [125] indicated that the TLR 4 gene in the lipopolysaccharide (LPS) chromosomal region was responsible for the defective LPS response. These authors also found that two LPS-hyporesponsive murine strains (C57BL-10/ScCr and C3H/HeJ) carried independent mutations in the TLR 4 genes, strongly suggesting that TLR 4 is critical for mediating reactions to LPS *in vivo* [125, 126]. TLR 4 can recognize LPS, moreover, it also binds some metal ions such as Co^{2+} and Ni^{2+} and several endogenous molecules (e.g., heat shock proteins) in humans [127-129]. Therefore,

periprosthetic inflammation is associated with TLR 4, which is regarded as a trigger of inflammatory pathways. However, some LPS is usually detected in the tissues around the aseptically loosened prosthesis; thus, controversy exists regarding whether the increased TLR 4 level is due to LPS in the periprosthetic tissues. Additionally, the changes in TLR 4 expression relevant to metallic particles and ionic products in periprosthetic tissues remain unclear.

1.4.4 TLR 5

TLR 5 is a transmembrane protein, which is located on the membrane of both immune and nonimmune cells [122]. Commonly, periprosthetic chronic inflammation caused by wear debris exerts a negative effect on the stability of implants. Some researchers have indicated that TLR 5 mediates in the process of inflammation-induced bone loss and osteoclastogenesis [130]. After the activation of TLR 5, receptor activator of nuclear factor kappa-B ligand (RANKL) is activated, eventually resulting in the upregulated expression of osteoclastic genes and subsequent osteoclast formation and bone loss. This process described above is absent in the TLR $5^{-/-}$ knockout mouse model [130]. Although TLR 5 is associated with bone loss, little is known about sterile inflammation in response to wear particles and metallic ions.

1.4.5 TLR 6

TLR 6, designated CD 286 (cluster of differentiation 286), usually functions in a heterodimer with TLR 2, mediating cellular responses to some viruses, fungi, gram-

positive bacteria, and even protozoa [131]. Additionally, TLR 6 also forms a heterodimer with TLR 4 to recognize endogenous ligands, modulating sterile inflammation [132, 133]. The recognition of zinc oxide nanoparticles by TLR 6 was shown to be a critical factor in the initiation of inflammatory reactions in macrophages [134]. Based on these discoveries, TLR 6 is also probably involved in aseptic implant loosening.

1.5 Outline, purpose, and hypothesis of this investigation

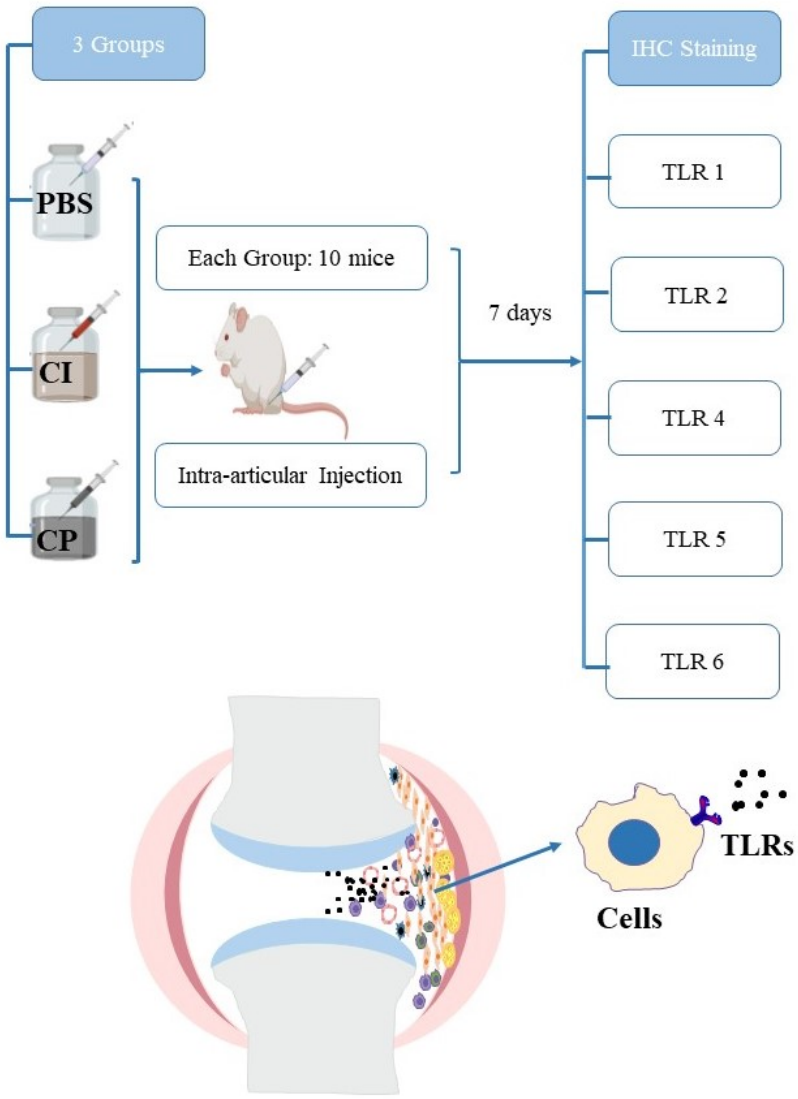

Figure 5. The experimental design of this *in vivo* study. Thirty mice are equally divided into three groups. The left knee joints of each group received intra-articular injection of PBS solution, CoCrMo particles, and CoCrMo ions, respectively. Immunohistochemistry staining was performed seven days after the injection. The expression levels of TLRs will be compared among these three groups. PBS, Phosphate-buffered saline; CI, CoCrMo ions; CP, CoCrMo particles; IHC, immunohistochemistry; TLRs, Toll-like receptors.

1.5.1 Experimental design

To date, the exact effects of specific Toll-like receptors (TLRs) in regulating

inflammatory reactions to CoCrMo particles and CoCrMo ions around orthopedic implants have not been fully clarified. Therefore, this study attempted to evaluate the expression of TLRs 1, 2, 4, 5, and 6 after CoCrMo particle and CoCrMo ion stimulation in the synovial layer *in vivo*. The experimental design is shown in Figure 5.

1.5.2 Aims of the study

The aim of this investigation was to determine the potential changes in cell surface receptors (specific TLRs) in response to CoCrMo particles (CP) and CoCrMo ions (CI) and to distinguish the difference in TLR expression levels between CoCrMo particles and ionic products in the murine knee joint synovial tissues.

1.5.3 The hypothesis

The hypothesis was created that the group injected with CoCrMo particles, and the CI group would express cell surface TLRs at higher levels compared to the control group. Because metal ions can function as haptens, the CI group would exhibit higher expression of specific TLRs compared to the CP group.

2. Materials and methods

2.1. CoCrMo particles/ions

As a part of the DFG-funded cooperative project, the production and analysis of CoCrMo particles and ionic products were finished by our cooperative team at University of Heidelberg. The metallic particles and metallic ionic products used in this study were generated from CoCrMo alloy samples according to ASTM F1537/ISO 5832–12. This type of wrought CoCrMo alloy is considered the standard material used in total joint replacements [135].

A wear test was performed using a custom-made pin-on-plate simulator to obtain CoCrMo particles. The frequency of the wear test was 1 Hz. A high-resolution inductively coupled plasma mass spectrometry (HR-ICP-MS) instrument (Thermo Scientific, Bremen, Germany) was used to determine the chemical composition of wear particles. Moreover, morphological parameters of wear particles, including the roundness (R), aspect ratio (AR), and equivalent circular diameter (ECD), were determined using scanning electron microscopy (SEM; Carl Zeiss, Oberkochem, Germany). The generated particle size and morphology were close to those of metallic particles obtained from revision surgeries [11, 136] **(Table 1)**.

Table 1. Morphological characters of metallic debris.

Materials	Roundness	Aspect ratio	ECD
CoCrMo alloy	0.64 ± 0.16	1.69 ± 0.66	61.25 ± 18.47 nm

The shape of produced particles: oval shape, 49%; rounded shape 44%; and needle shape, 7 %.

A CoCrMo alloy specimen was eroded in a corrosion measuring cell to generate CoCrMo ions. A PBS solution was used as the surrounding medium. The chemical composition of CoCrMo ions was determined utilizing an HR-ICP-MS (Thermo Scientific, Bremen, Germany) instrument. The concentration of all dissolved metallic ions in the PBS solution was detected as 20.5 mg/L, which was subsequently diluted to the setting concentration (200 µg/L) **(Table 2)**. The selected concentration (200 µg/L) was determined from an examination in which the patient's joint puncture was analyzed before the revision arthroplasty (in the case of MoM bearing couples). Median concentrations ranging from 200-250 µg/L were measured [137].

Table 2. Metallic ion concentrations in the PBS solution

Element	Co	Cr	Mo	Ni
Concentration(mg/L)	13.7	4.3	0.8	1.7

The total concentration of CoCrMo ionic solution were determined as 20.5 mg/L.

2.2. Removal of endotoxins

TLR activation in the synovium will be observed after CoCrMo particles and ions are injected into the knee joints. Prior to the animal experiments, PAMPs, such as lipopolysaccharides, must be removed from CoCrMo particles and CoCrMo ions to avoid relevant interference factors. Thus, an ethanol washing procedure was used to clean the generated particles, whereas a heat-shock method was carried out to treat the

metallic ions. The Limulus amebocyte lysate assay (Lonza, Cologne, Germany) was used to examine the efficiency of endotoxin removals.

2.3 *In vivo* trials: mice and intra-articular injections

30 female Balb/c mice obtained from Charles River Laboratories (Sulzbach, Germany) were used in this investigation. The weight range of these mice was 18-25g. All mice were randomly assigned into one of the following three groups: the group injected with CoCrMo particles (CP group, n = 10), the group injected with CoCrMo ions (CI group, n = 10), and the group injected with PBS solution (control group, n = 10).

Before the intra-articular injection procedure, the solution designated for each group was treated with ultrasound for 60 minutes to avoid possible aggregation and precipitation. Subsequently, 50 μL of a 0.1 vol% CP suspension, 50 μL of 200 μg/L CI solution, and 50 μL of the PBS solution were released into the joint cavity of murine left knee by injectors under sterile conditions. Seven days later, all mice were sacrificed by an overdose of pentobarbital (Merial, Hallbergmoos, Germany). All knee joints were removed for subsequent immunohistological analyses.

For *in vivo* trials, the intra-articular injection of mice was performed by my colleague, Dr. med. Kathrin Ebinger. There is no conflict of interest. All experimental procedures relevant to mice were conducted in accordance with the European Directive 2010/63/EU Act and the rules of the Animal Protection Laboratory Animal Regulations

(2013) and approved by the Upper Bavaria government, Germany (protocol number: 55.2-1-54-2532-82.12).

2.4 Immunohistochemistry (IHC)

2.4.1 Paraffin blocks and sections

After the samples of murine knee joints were collected, all knee samples were fixed with 4% formaldehyde at room temperature, followed by decalcification in Osteosoft® solution (Merck, Darmstadt, Germany). Subsequently, the decalcified samples were dehydrated in a series of rising ethanol concentrations (70%, 96%, 100%, and xylene) by a Spin Tissue Processor 120 instrument (Myr, Tarragona, Spain) and finally successively transferred to two paraffin wax baths at about 60 °C.

After the dehydration step, the embedding cassettes containing knee samples were transferred to a paraffin embedding station (Leica Microsystems, Nussloch, Germany). An appropriate mold was selected and then filled with paraffin as required. Later, the knee sample was transferred from the cassette to the mold. Using forceps, the knee sample was oriented parallel to the cut surface. After the orientation of the knee sample, the mold was filled with paraffin. Finally, the mold with the paraffin block was placed on the cold plate until all the paraffin was fully solidified. The paraffin blocks were then removed from the molds and stored at room temperature until further processing.

Paraffin blocks were placed on a cold plate (-20 °C) before sectioning. Cold wax

provides support for hard elements within the tissue specimen, and thus thin sections are easy to obtain. The thickness of sections was 3 μm. After the cutting process, the section was picked up with forceps and moved to a water bath (38 °C). The warm water helped remove wrinkles from the section. Then, the sections were mounted on labeled slides. Finally, the labeled slides were placed on a heating plate and incubated at 65 °C for approximately one hour to evaporate water and melt the wax of sections. The slides were then stored in slide boxes.

2.4.2 IHC staining procedure

The prepared tissue sections were examined immunohistochemically using five anti-mouse polyclonal antibodies against TLRs 1, 2, 4, 5, and 6. Each antibody was used separately in the formal experiments. Thirty samples, including samples from the CP group (n = 10), the CI group (n = 10), and the PBS group (n = 10), were stained simultaneously as one batch in each staining process to avoid differences in staining between batches. The knee sample to which the primary antibody was not added was regarded as the no primary antibody control (NC). The splenic sample rich in TLRs was considered as the positive control in this study. False-positive staining and false-negative staining were avoided by analyzing NC and positive controls. After every step using reagents during the staining period, tissue sections were washed with washing buffer three times. The washing buffer was composed of 5 L of PBS and 5 mL of Brij. All prepared buffers and solutions used in the staining process are listed in **Table 3**

Table 3. Prepared buffers and solutions

Name	Preparation method
PBS buffer (1 x)	1 liter of PBS buffer (10 x concentrated) + 9 liters of distilled water
Hydrogen peroxide 3%	20 mL 30% H_2O_2 + 180 ml deionized water
PBS-Brij (washing buffer)	5 liters of diluted PBS (1 x) buffer + 5 ml Brij
EDTA buffer (pH 9.0)	10 mL EDTA (pH 9.0; 10 x) + 90 mL deionized water
Citrate buffer (pH 6.0)	10 mL citrate buffer (pH 6.0; 10 x) + 90 mL deionized water
EDTA buffer (pH 8.0)	10 mL EDTA (pH 8.0; 10 x) + 90 mL deionized water
Chromogenic approach	1000 µL DAB substrate buffer + 1 drop DAB concentrate
Antibody approach 1: 50	100 µL primary antibody + 4.9 mL Antibody dilution buffer

Before IHC, specific slides were placed at 60 °C for one hour to melt the wax on the slides. Then, the slides were dewaxed in xylene for 20 minutes and rehydrated via a descending alcohol series (100% 2 x 10 min, 96% 5 min, 70% 5 min, finally in distilled water). All wax must be removed to allow aqueous solutions to penetrate the sections. Background staining was sometimes also due to the existence of wax pots, and thus this step was essential.

2.4.2.1 Heat-induced epitope retrieval (HIER)

Formalin-fixed samples usually require an antigen retrieval step. Commonly, methylene bridges will be formed during formalin fixation and cover antigenic sites. These methylene bridges can be broken, and antigenic sites can be exposed again via antigen retrieval procedures [138]. Enzymatic retrieval and heat-induced epitope

retrieval (HIER) are two methods for antigen retrieval. Because the section morphology is easily damaged by the enzymatic retrieval method, we decided to use the HIER method. There are three kinds of buffer solutions used for HIER in this investigation: EDTA buffer (pH 8.0), citrate buffer (pH 6.0), and EDTA buffer (pH 9.0; DCS, Hamburg, Germany). Based on the results of a pretest, EDTA (pH 8.0) buffer was used in our formal experiments. The appropriate antigen retrieval buffer with samples was placed in a pressure cooker (2100-Antigen Retriever, BioVendor GmbH; Kassel, Germany) for thirty minutes. After removal from the pressure cooker, slides were placed in the buffer for approximately one hour until slides turned back to room temperature.

2.4.2.2 Endogenous peroxidase blocking

For the chromogenic procedures in IHC, an enzyme is usually linked to secondary antibodies to visualize antibody localization [139]. If the enzyme also exists in the targeted tissue, its reaction must be blocked before the chromogenic step. In this study, we used horseradish peroxidase (HRP) to conduct the chromogenic procedure, and thus endogenous peroxidase activity must be blocked to avoid the non-specific background staining. All tissue samples were immersed with 3% hydrogen peroxide (Merck KGaA, Darmstadt, Germany) for ten minutes to block endogenous peroxidase activity after the HIER step in this investigation.

2.4.2.3 Antibody incubation and chromogenic procedures

Serial dilution pretests should be conducted to obtain the optimized dilution of each primary antibody before the formal experiment and to avoid overstaining or very weak staining of the tissue sections. Therefore, a dilution ratio gradient-related analysis was carried out before the formal experiments. By adding antibody dilution buffer, the concentrated solution of primary antibodies was diluted to 1:150, 1:200, 1:300, 1:400, and 1:500. Then, all diluted solutions of each antibody were simultaneously tested for IHC staining. After the analysis of IHC staining density, the optimized dilution for each primary antibody would be obtained. The optimized dilution will be shown in the result parts. The basic information of primary antibodies was shown as below **(Table 4**).

Table 4. Basic information of primary antibodies

Primary Antibodies (Rabbit anti-mouse polyclonal antibodies)	Stock solution	Source
TLR 1 antibody	100 µL	Biorbyt Ltd., UK, Cat no.: orb 48968
TLR 2 antibody	100 µL	Biorbyt Ltd., UK, Cat no.: orb 11487
TLR 4 antibody	100 µL	Biorbyt Ltd., UK, Cat no.: orb 11489
TLR 5 antibody	100 µL	Biorbyt Ltd., UK, Cat no.: orb 11490
TLR 6 antibody	100 µL	Biorbyt Ltd., UK, Cat no.: orb 252521

In the formal staining procedures, the slides were quickly removed from the washing buffer and placed in a humidified chamber. Then, they were incubated with 150 µL of diluted primary antibodies at room temperature (20-22 °C) for one hour. When the

incubation with the primary antibodies was finished, the SuperVision 2 HRP-Polymer system kit (DCS, Hamburg, Germany) was used to bind primary antibodies according to the manufacturer's protocol. Subsequently, DAB substrate (DCS, Hamburg, Germany) was freshly prepared as a chromogen to visualize the antigen-antibody interactions. The chromogenic procedure was completed in three minutes. Later, all tissue sections were counterstained with Mayer's hematoxylin (Morphisto GmbH, Frankfurt, Germany) for one minute. After the counterstaining, all slides were placed in running tap water for bluing (pH 7.5). Then, the sections were dehydrated in a series of rising ethanol concentrations (70%, 96%, 100%, and finally in xylene). Finally, all histology slides were mounted using cover-glasses and EUKITT (O. Kindler GmbH, Freiburg, Germany).

A PreciPoint M8 microscope (Freising, Germany) was used to image the stained sections at 200-fold magnification. The synovial tissue represents the region of interest (ROI) in this study. Images including most of the synovial layer were captured for the subsequent quantitative analysis. If cells of the synovial membrane displayed a brown or deep yellow color and the nucleus had a blue color, positive staining was recorded. Two investigators individually counted positive cells using Image J software (Bethesda, MD, USA). Finally, the mean value was calculated to perform the subsequent histomorphometrical analysis.

2.5 Statistical evaluation

The data obtained from the manual counts were evaluated with GraphPad Prism 8.3.0 (GraphPad Software, San Diego, USA). The Shapiro-Wilk test and the Anderson-Darling test were used to determine the distribution of the data. With regard to data having a normal distribution, the one-way analysis of variance (ANOVA) was used to evaluate whether there was a significant difference for the three independent groups in this study. As a follow-up test to ANOVA, the Tukey test was used to compare significant differences between every group with every other group. If the data failed the normality test, the Kruskal-Wallis test was conducted in this investigation. As a post-test following a Kruskal-Wallis test, the Dunn's test was used to compare significant differences between every group with every other group. The results are presented in box plots. A P-value < 0.0167 (Bonferroni adjustment) was regarded to be statistically significant.

3. Results

3.1 Pretests

3.1.1 Positive controls

The spleen, an immune organ, expresses all antigens that were our focus in this study. Therefore, splenic tissue was used as a positive control. In the pilot experiment, positive reactions were detected in the splenic tissue after IHC staining was conducted using anti-TLR 1, 2, 4, 5, and 6 polyclonal antibodies. These pretests indicated that the staining assay was working correctly. In the subsequent formal experiments, one splenic sample was stained again in each staining batch to avoid false-negative results. Additionally, one splenic sample to which the primary antibody was not added was also included in each staining batch to avoid nonspecific staining and false-positive results. No positive staining was observed when the no-primary-antibody-control (NC) was used in this study. The representative images are shown **in Figure 6.**

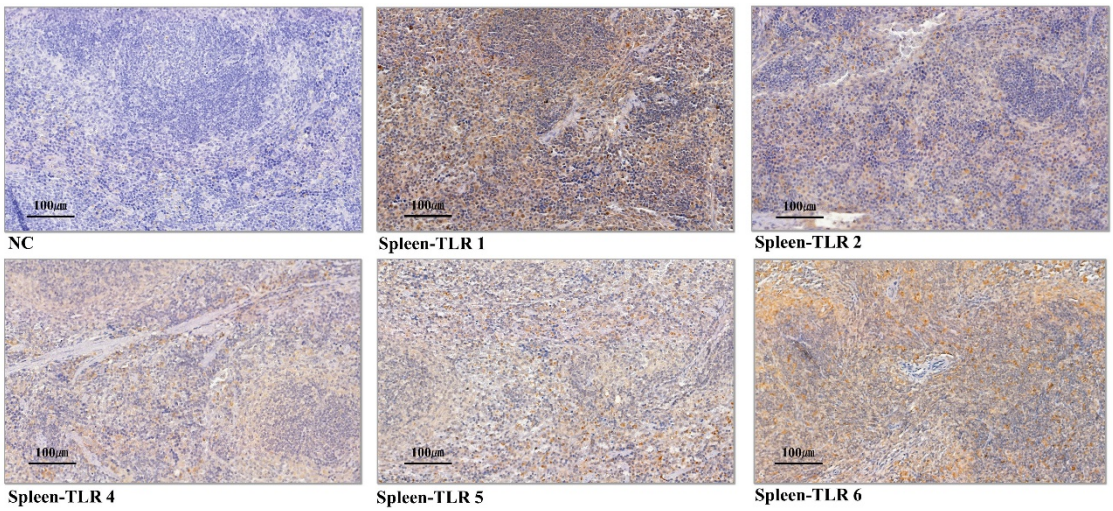

Figure 6. Representative images of positive controls. The splenic tissue expresses all surface TLRs we used in this study. So, the splenic tissue was regarded as the positive control. NC, no primary antibody control. TLRs 1, 2, 4, 5 and 6, Toll-like receptors 1, 2, 4, 5 and 6. (Scale bar = 100 μm).

3.1.2 Optimal pH of HIER

The optimal pH of heat-induced antigen retrieval must be determined experimentally. Three reagents, EDTA buffer (pH 8.0), citrate buffer (pH 6.0), and EDTA buffer (pH 9.0; DCS, Hamburg Germany), were tested in the pilot study. After the staining procedures, positive reactions were observed when we used these three types of reagents (pH 6.0, 8.0, and 9.0). After the comparison, EDTA buffer pH 8 was regarded as the optimal pH. As shown in the figure below **(Figure 7)**, when EDTA buffer pH 8 was used, positive reactions and almost no background staining were observed.

Therefore, EDTA buffer (pH 8) was considered to be the optimal reagent for heat-induced antigen retrieval in the subsequent experiments. No positive reaction was detected in the sample incubated without a primary antibody (NC). This NC sample

helped to exclude false-positive results.

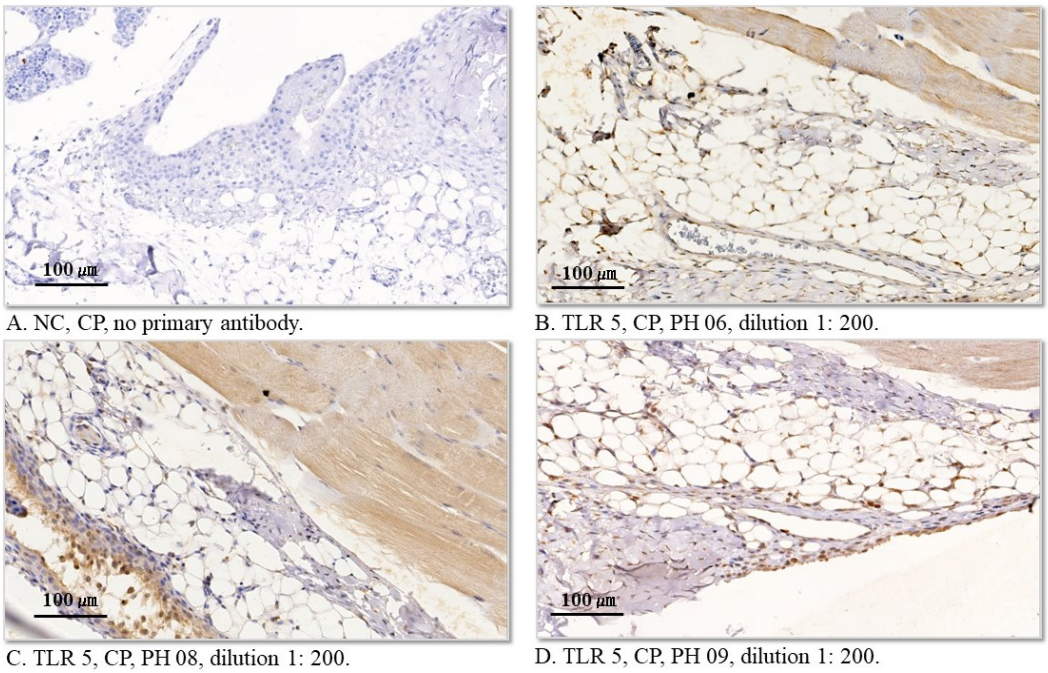

A. NC, CP, no primary antibody.

B. TLR 5, CP, PH 06, dilution 1: 200.

C. TLR 5, CP, PH 08, dilution 1: 200.

D. TLR 5, CP, PH 09, dilution 1: 200.

Figure 7. Effect of pH on heat-mediated antigen retrieval in the synovial tissue. A, NC, no primary antibody control. B, the TLR 5 expression using citrate-buffer pH 6 in the murine knee joint synovium. The dilution ratio is 1:200, which is based on the product-sheet of TLR 5. C, the TLR 5 expression using EDTA buffer pH 8 in the murine knee joint synovium. D, the TLR 5 expression using EDTA buffer pH 9 in the murine knee joint synovium. NC, no primary antibody control. TLR 5, Toll-like receptor 5. CP, the CoCrMo particle sample. (Scale bar = 100 μm).

3.1.3 Primary antibody optimization

The quality of IHC staining is also influenced by the dilution ratio of the primary antibody. This dilution ratio of each primary antibody must be optimized in different tissues to ensure specific staining with minimal background staining. We found that the staining intensity decreased with decreasing concentrations of the antibody solution, based on the staining results. In the representative images shown in **Figure 8**, when the dilution ratio of TLR 4 was 1:200, the best effect of staining was observed. Therefore, for TLR 4, we used a dilution ratio of 1:200 in the subsequent experiment. The

optimized dilution related to each primary antibody is shown in **Table 5**.

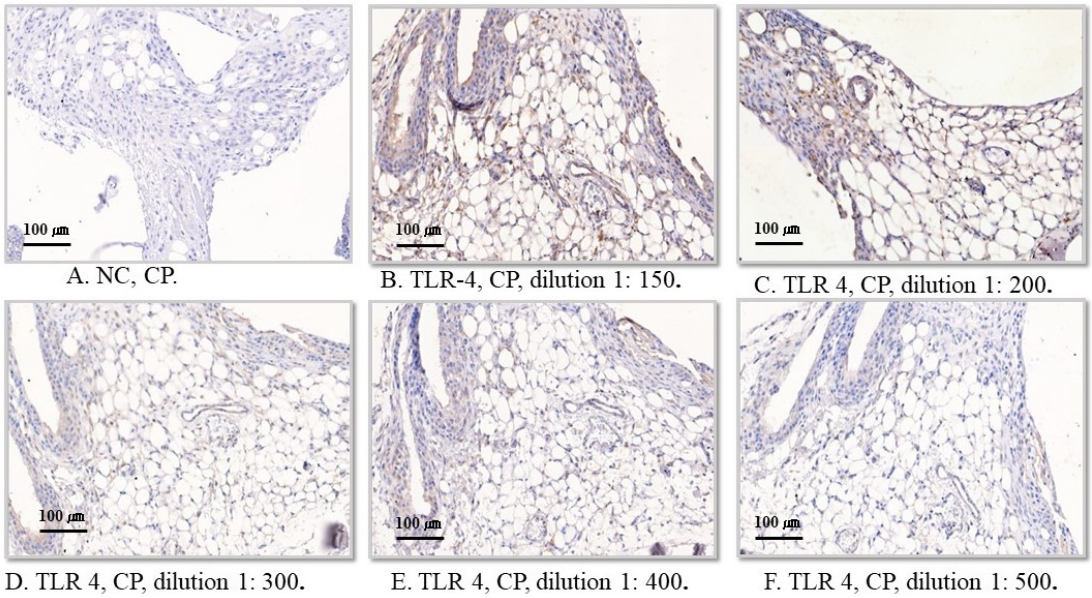

Figure 8. The dilution ratio gradient-related analysis for TLR 4 antibodies. A, no primary antibody is added. B, C, D, E, and F represent images that the concentrated solution of primary antibodies is diluted 150, 200, 300, 400, and 500 times, respectively. NC, no primary antibody control. TLR 4, Toll-like receptor 4. CP, the CoCrMo particle sample. (Scale bar = 100 μm).

Table 5. The optimized dilution ratio for each primary antibody

TLRs	Dilution	Manufacturer
TLR 1 antibody	1:500	Biorbyt Ltd., Cambridge, United Kingdom
TLR 2 antibody	1:200	Idem
TLR 4 antibody	1:200	Idem
TLR 5 antibody	1:300	Idem
TLR 6 antibody	1:200	Idem

3.2 Expression of TLRs

3.2.1 Expression of TLR 1

With regard to the CP group, a large number of round macrophage-like cells were observed in the central region of the thickened synovial tissue. Most of the round cells were positively stained with TLR 1 antibodies. Moreover, many spindle-shaped, fibroblast-like cells were also observed, especially in the marginal area of the thickened synovial tissue. Some of the fibroblast-like cells displayed positive staining with TLR 1 antibodies **(Figure 9A, CP-TLR 1)**. In the CI group, numerous positively stained cells with TLR 1 antibodies could be observed in the synovium. A representative image of the CI group showed a hyperplastic synovium that tend to "invade" the neighboring adipose tissue **(Figure 9A, CI-TLR 1)**. There was no clear border between the synovial layer and the adjacent adipose tissue. Some positively stained cells with TLR 1 antibodies could be found around the capillaries of the thickened sub-synovial tissue in the image. In the control group, only scattered positive stained cells were observed in the synovium.

According to the histomorphometrical analysis, the CP group had a median of 192.5 positive cells per visual field (min. 78.3; max. 232.2 positive cells/visual field). The CI group showed a median of 73.75 positive cells per visual field (min. 44.2; max. 114 positive cells per visual field). The control group showed a median of 37.5 positive cells per visual field (min. 7.25; max. 100.8 positive cells per visual field). The analysis of these data indicated that cells that showed positive staining with TLR 1 antibodies in the CP group had significantly higher numbers than those in the CI group and the PBS

group ($p < 0.0167$); however, cells with positive staining in the CI group did not show a noticeable difference compared with the PBS group (**Figure 9B).**

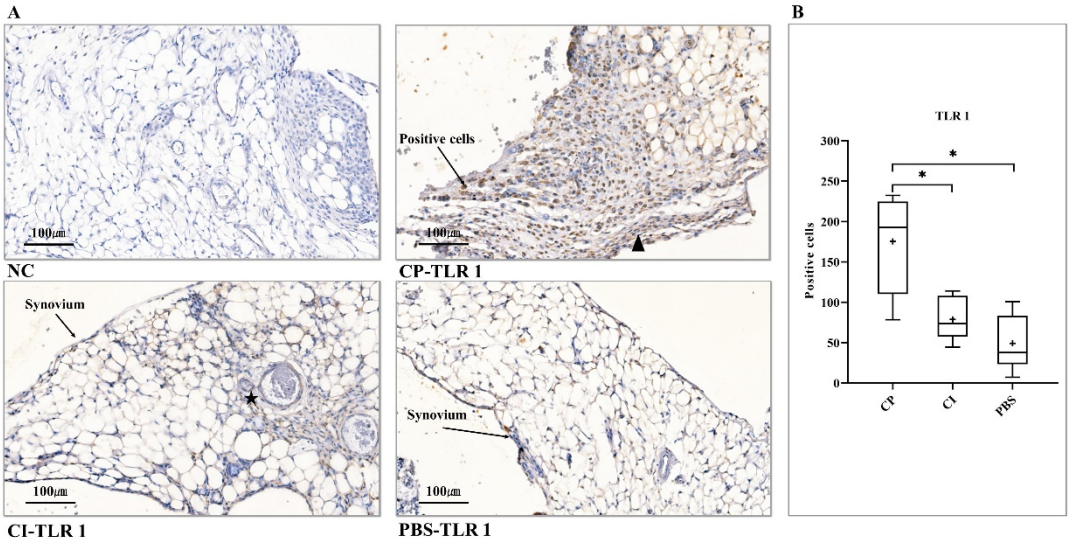

Figure 9. IHC staining results of TLR 1 in the murine knee joint synovial tissue. (A) NC, no positively stained cells. CP-TLR 1, numerous positively stained cells can be observed. Black arrow, round macrophage-like cells; triangle (▲), spindle-shaped fibroblast-like cells. CI-TLR 1, some positively stained cells can be observed. Pentagram (★), the capillary in the neighboring adipose tissue. PBS-TLR 1, few positively stained cells are observed. (B) Statistical analysis of TLR 1 [One way analysis of variance (Tukey's test)]. IHC, immunohistochemistry; PBS, phosphate-buffered saline; NC, no primary antibody control; CP, CoCrMo particles; CI, CoCrMo ions; TLR, Toll-like receptor. (* = $p < 0.0167$; Scale bar = 100 µm).

3.2.2 Expression of TLR 2

Concerning both the CP group and the CI group, hyperplastic synovial tissues were observed under the microscopy. Many positively stained cells with TLR 2 antibodies were found in both the CP and CI groups. In the control group, only scattered cells showed positive staining with TLR 2 antibodies **(Figure 10A)**.

In the histomorphometrical analysis, the CP group exhibited a median of 99.2 positive

cells per visual field (min. 41.5; max. 150.5 positive cells per visual field). The CI group showed a median of 34.58 positive cells per visual field (min. 21; max. 89.25 positive cells per visual field). The PBS group displayed a median of 14.38 positive cells per visual field (min. 2.2; max. 53.4 positive cells per visual field). Based on the results of the histomorphometrical analysis, only the CP group showed significantly increased positive cells with TLR 2 antigens in comparison with the PBS group ($p < 0.0167$) **(Figure 10B).**

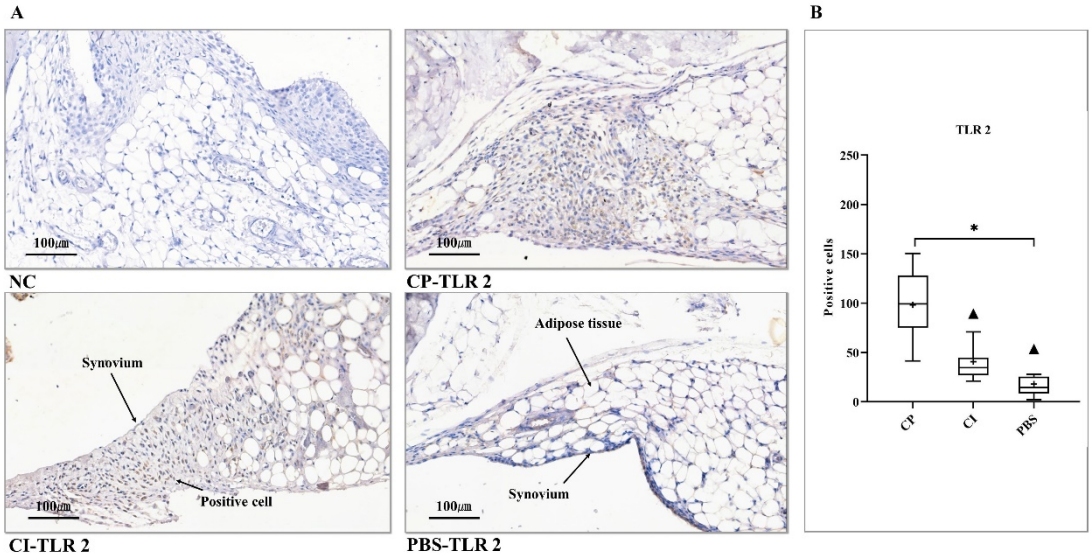

Figure 10. IHC staining results of TLR 2 in the murine knee joint synovial tissue. (A) NC, no positively stained cells. CP-TLR 2 presented many positively stained cells and thickened synovium. CI-TLR 2, some cells are positively stained in the thickened synovial membrane. PBS-TLR 2, few cells are positive in the synovial membrane. (B) Statistical analysis of TLR 2 [Kruskal Wallis test (Dunn's test)]. IHC, immunohistochemistry; PBS, phosphate-buffered saline; NC, no primary antibody control; CP, CoCrMo particles; CI, CoCrMo ions; TLR, Toll-like receptor. (* = $p < 0.0167$; Scale bar = 100 µm).

3.2.3 Expression of TLR 4

In the CP group, a thickened synovial layer and apparent inflammatory cell infiltrates were observed. Additionally, many inflammatory cells invaded the adjacent adipose

tissue. Numerous fibroblast- and macrophage-like cells were observed in the infiltrated region; most of them were positively stained with TLR 4 antibodies. In the CI group, many cells having positive staining were also found in the hyperplastic synovium; however, only scattered cells that showed positive staining with TLR 4 antibodies were detected in the PBS group **(Figure 11A)**.

Based on the histomorphometrical analysis, the CP group had a median of 96.53 positive cells per visual field (min. 67.25; max. 157.25 positive cells per visual field). The CI group showed a median of 68.65 positive cells per visual field (min. 28.5; max. 125.3 positive cells per visual field. The PBS group presented a median of 29.7 positive cells per visual field (min. 7.25; max. 72.5 positive cells per visual field). According to these TLR 4 data, the number of cells with positive staining in the CP group had considerable differences only the CP group showed significantly increased positive cells with TLR 2 antigens in comparison with that in the CI group and the PBS group. Meanwhile, the CI group demonstrated higher TLR 4 expressions than the PBS group ($p < 0.0167$) **(Figure 11B).**

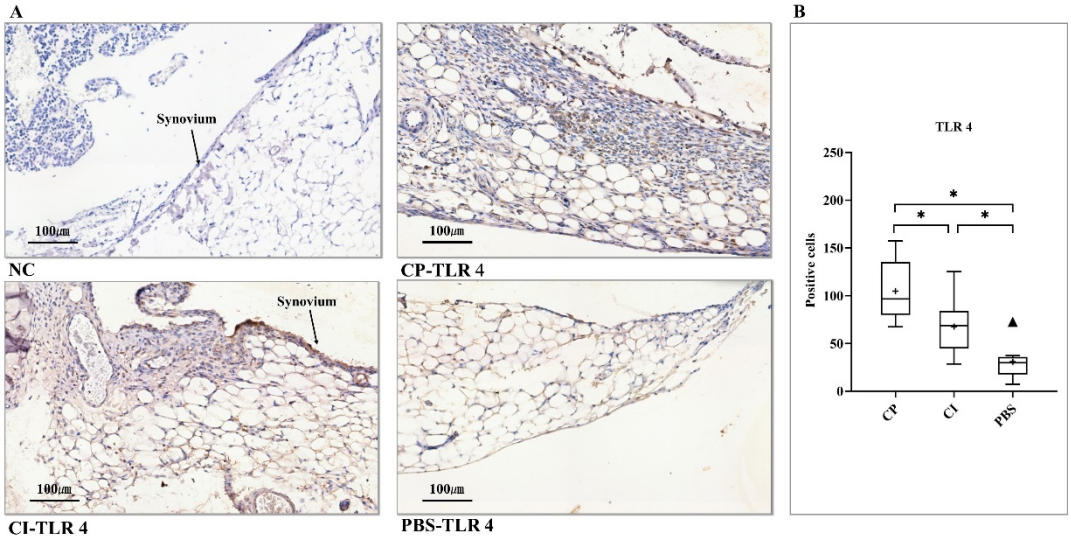

Figure 11. IHC staining results of TLR 4 in the murine knee joint synovial tissue. (A) NC, no positively stained cells. CP-TLR 4, dense inflammatory cell infiltrates are found in the thickened synovial membrane. Obvious adjacent adipose tissue loss are observed. CI-TLR 4, some positively stained cells are found in the synovial tissue. PBS-TLR 4, only scattered positively stained cells are observed in the synovial tissue. (B) Statistical analysis of TLR 4 [One way analysis of variance (Tukey's test)]. IHC, immunohistochemistry; PBS, phosphate-buffered saline; NC, no primary antibody control; CP, CoCrMo particles; CI, CoCrMo ions; TLR, Toll-like receptor. (* = $p < 0.0167$; Scale bar = 100 µm).

3.2.4 Expression of TLR 5

Following stimulation with CoCrMo particles, newly formed granulation tissue was observed in the CP group, which was quite close to the granulomatous tissue (pseudotumor) obtained from patients who received revision arthroplasty. Additionally, with the formation of granulation structures in the CP group, the wide-ranging neighboring adipose tissue seemed to disappear (**Figure 12A, CP-TLR 5)**. While no granulation structure was observed in the CI group, a thickened synovial membrane was found **(Figure 12A, CI-TLR 5)**.

In the histomorphometrical analysis, the CP group had a median of 133.4 positive cells per visual field (min. 37.4; max. 171 positive cells per visual field). The CI group displayed a median of 44.63 positive cells per visual field (min. 18.5; max. 84.5 positive cells per visual field). A median of 21 positive cells per visual field (min. 11.25; max. 66.5 positive cells per visual field) was detected in the PBS group. Based on these data above, only the CP group displayed numerous cells that had positive staining with TLR 5 antibodies in comparison with the PBS group ($p < 0.0167$) **(Figure 12B).**

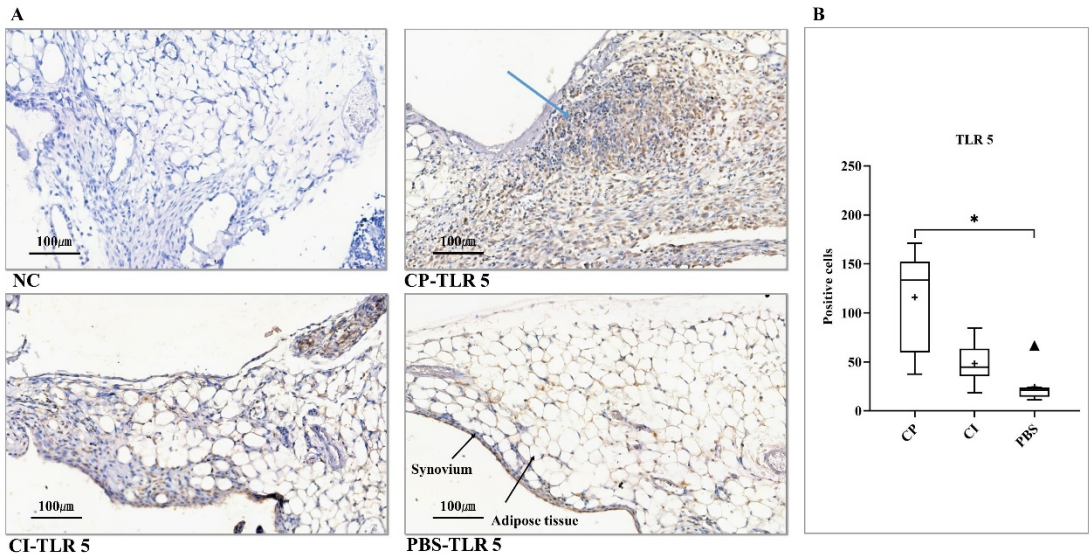

Figure 12. IHC staining results of TLR 5 in the murine knee joint synovial tissue. (A) NC, no positively stained cells. CP-TLR 5, blue arrow, the granulation tissue is found in the synovial tissue. CI-TLR 5, some positively stained cells are found in the synovial tissue. PBS-TLR 5, few cells show positive staining in the synovial tissue. (B) Statistical analysis of TLR 5 [Kruskal Wallis test (Dunn's test)]. IHC, immunohistochemistry; PBS, phosphate-buffered saline; NC, no primary antibody control; CP, CoCrMo particles; CI, CoCrMo ions; TLR, Toll-like receptor. (* = $p < 0.0167$; Scale bar = 100 µm).

3.2.4 Expression of TLR 6

Necrotic tissue caused by CoCrMo particles was displayed in the CP group. Black CoCrMo particles, green corrosion CoCrMo particles, inflammatory cell infiltrates, and numerous fibroblast-like cells could be observed in the necrotic tissue **(Figure 13A,**

CP-TLR 6). Typically, in the tissue retrieved from revision surgeries, corrosion CoCrMo particles appear greenish, while conventional CoCrMo particles are mainly black [41]. Therefore, the clinically observed CoCrMo particles are similar with particles that we detected in the necrotic tissue in the present study. In the CP group, many cells that showed positive staining with TLR 6 antibodies were found around the necrotic tissue. Additionally, numerous cells with positive staining were also observed in the apparent hyperplastic synovium of the CI group **(Figure 13A, CI-TLR 6)**.

Based on the histomorphometrical analysis, a median of 142.6 positive cells per visual field (min. 74.3; max. 205 positive cells per visual field) was detected in the CP group. The CI group showed a median of 74.42 positive cells per visual field (min. 45; max. 99.4 positive cells per visual field). A median of 33.3 positive cells per visual field (min. 15.8; max. 72.75 positive cells per visual field) was found in the PBS group. In terms of the statistical analysis, the number of cells that showed positive staining with TLR 6 antibodies in the CP group had considerable differences in comparison with that in the CI group and control group (PBS). Meanwhile, the CI group presented more positive cells than the control group ($p < 0.0167$) **(Figure 13B)**

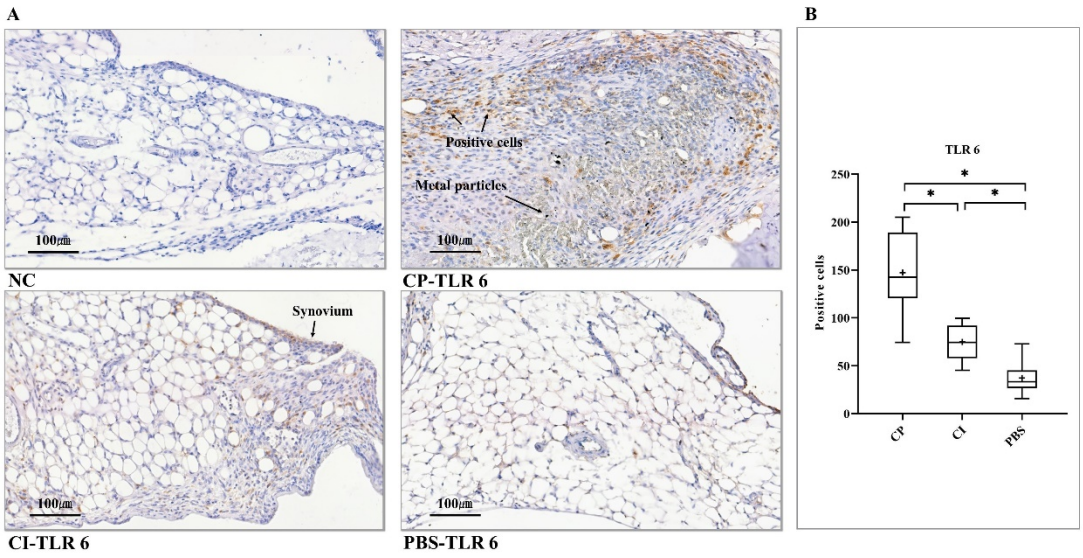

Figure 13. IHC staining results of TLR 6 in the murine knee joint synovial tissue. (A) NC, no positively stained cells. CP-TLR 6, black CoCrMo particles and green corrosion particles are found in the necrotic tissue. CI-TLR 6, numerous positively stained cells are found in the thickened synovial tissue. PBS-TLR 6, scattered cells show positive staining in the synovial tissue. (B) Statistical analysis of TLR 6 [One way analysis of variance (Tukey's test)]. IHC, immunohistochemistry; PBS, phosphate-buffered saline; NC, no primary antibody control; CP, CoCrMo particles; CI, CoCrMo ions; TLR, Toll-like receptor. (* = $p < 0.0167$; Scale bar = 100 µm).

3.3 Graphical summary

Immunohistochemical staining was carried out in the knee joint synovial tissue of a mouse model. Anti-TLR 1, 2, 4, 5, and 6 antibodies were used to detect target proteins on dewaxed synovial tissue sections. Increased inflammatory cell infiltrates and a hyperplastic synovial layer were observed in both the CP and CI groups. Additionally, the CP group presented significantly upregulated TLR expression compared with the PBS group and an elevated number of cells that had positive staining with TLR 1-, 4-, and 6-antibodies in comparison with the CI group ($p < 0.0167$). The CI group showed significantly higher levels TLRs 4 and 6 expression than the control group. Greenish

corrosion particles were observed in the necrotic tissue, suggesting that CoCrMo particles might release a certain level of locally toxic metallic ions *in vivo* **(Figure 14)**.

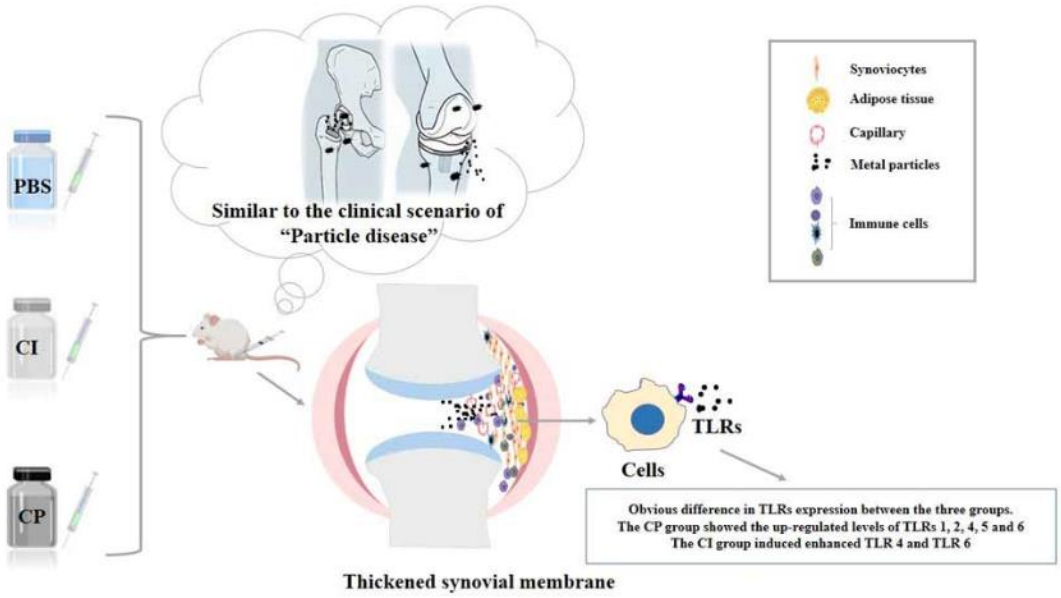

Figure 14. Graphical summary of this study. CP, CoCrMo particles; CI, CoCrMo ions; TLR, Toll-like receptor; PBS, phosphate-buffered saline.

4. Discussion

The acquired IHC results partially controverted the initial hypothesis. The CP group, rather than the CI group, had significantly higher levels of all TLRs used in this investigation than the control group. Even dramatically upregulated TLR 1, 4, and 6 expressions were observed in the CP group in comparison with the CI group. Only higher TLR 4 and 6 expressions were detected in the CI group than those in the control group. In the next section, the inflammatory animal model and TLR results will be discussed retrospectively.

4.1 The inflammatory model *in vivo*

After total hip arthroplasty [2], adverse local tissue reactions (ALTRs) caused by abrasion products remain one common cause for revision operations in the middle- and long-term [13, 140]. The synovial-like interface membrane around implants is the central effector region of adverse reactions to abrasion products and has attracted much attention from the scientific community [141]. Some researchers have tried to use some histological methods and leukocyte/endothelial-cell interactions to measure the biological responses to wear debris in the murine synovial layer [79]. Migration of leukocytes from lymphatic or blood vessels into tissues occurs more extensively in the presence of inflammatory reactions or injuries in local tissue sites. Therefore, based on leukocyte-endothelial cell interactions measured using intravital microscopy, the extent of the biological responses caused by wear debris can be determined [79]. Additionally, the thickened synovial layer and inflammatory cell infiltration can also be measured via

a histological analysis.

Zysk et al. [142] were the earliest researchers to utilize this murine model to evaluate biological reactions caused by wear particles. Some Balb/c mice received intra-articular injections of wear particle suspensions. Seven days after the wear particle injection, leukocyte-endothelial cell interactions and histological sections were observed to determine the extent of inflammatory reactions. This significant step achieved with this murine model is an intra-articular injection of wear particles. This procedure mimics the intra-articular release of abrasion products from implants and the debris distribution in the knee joints. After the animal model was established, Zysk et al. [142] primarily observed the effect of the debris composition. They found that titanium particles, polyethylene particles, and polymethyl methacrylate (PMMA) particles caused considerably intensified leukocyte-endothelial cell interactions and stronger pro-inflammatory responses compared with the control group. The same researchers subsequently used this murine model to evaluate the influence of debris sizes on inflammatory responses [143]. They indicated that smaller polystyrene wear fragments (0.5 and 2.0 μm) caused a more severe pro-inflammatory reaction than large ones (75 μm) at the same volume [143]. Afterward, Utzschneider et al. [144] compared polyether-ether-ketone (PEEK) particles with ultrahigh-molecular-weight-polyethylene (UHMWPE) particles in the same murine model. These authors did not observe an obvious difference between PEEK and UHMWPE particles. Thus, these two kinds of particles might induce a comparable inflammatory response *in vivo*.

Based on the studies mentioned above, in this investigation, we tried to evaluate the expression levels of TLRs in the synovial layer after CoCrMo particles and CoCrMo ions were injected into the murine knee joints. Commonly, the sterile inflammatory responses caused by wear debris are considered the central biological reactions around implants [145]. TLRs, which are single-pass membrane-spanning proteins, play a critical role in triggering sterile inflammation [111]. According to some studies, wear debris-induced inflammation might be mitigated by a specific pharmacological blockade of one TLR or more TLRs [117]. Similarly, TLRs have become therapeutic targets for many other diseases. Some synthetic or biological antagonists have been developed to regulate TLR function. According to the literature, the surfactant protein-A-derived (SPA4) peptide has been used to suppress the inflammatory response in the lung by blocking the activated TLR 4 [146]. Some DNA-based small molecules, such as IMO-3100, have been used to treat psoriasis by binding to TLR 7-9 [147]. Based on these discoveries, the expression levels of distinct TLRs, including TLRs 1, 2, 4, 5, and 6, were evaluated in the murine knee joint synovial tissue in the present study. TLRs 1, 2, 4, 5, and 6 are expressed both in humans and mice. Additionally, they are mainly expressed on the cellular surface, increasing the possibility of direct interactions between wear debris and TLRs, so these receptors are selected in this study.

This study aims to identify the potential cell surface TLRs with higher expression after CoCrMo particle and CoCrMo ion stimulation. The differences in TLR expression

between animals injected with CoCrMo particles and CoCrMo ions are clarified. We hope that our study provides a helpful reference for designing therapeutic agents for inflammatory reactions to CoCrMo particles and ionic products in the synovial-like interface membrane.

Immunohistochemical (IHC) staining detects the presence and location of specific proteins in synovial tissues [41]; additionally, IHC enables the quantification of cells expressing particular proteins in the context of intact synovial tissues [141]. Therefore, IHC techniques were used to detect TLR-positive cells in synovial tissue in this study. After IHC staining, black CoCrMo particles, green corrosion CoCrMo particles, necrotic tissues, inflammatory cells, and even granulomatous tissues were found in the murine knee joint synovial tissues in this study. These tissue characteristics are highly close to periprosthetic tissues obtained from revision surgeries [6, 27, 41, 59].

In clinical studies, standardized IHC analyses also plays a vital role in understanding the synovial-like interface membrane inflammatory characteristics around implants [148]. The quantification of specific cell categories via IHC techniques has been used to determine potential thresholds for some pathological responses around implants, such as the diagnosis of low-grade bacterial infections by counting CD15 positive cells [141]. However, a sufficient amount of periprosthetic tissue samples is difficult to obtain from revision surgeries to perform relatively basic studies. The established murine model provides a calculable number of synovial tissues. Furthermore, based on

the highly similar tissue characteristics between the synovium and synovial-like tissue around implants [142], the established murine model might be able to further analyze biological reactions caused by wear debris.

Numerous *in vitro* cell culture models have also been used to study sterile inflammation caused by wear debris [149-151]. *In vitro* models allow the representation of the inflammatory reaction in a specific cell line upon particle stimulation. However, for actual debris-induced inflammatory responses *in vivo*, various types of cells, mainly including macrophages, fibroblasts, endothelial cells, lymphocytes, neutrophils, and mast cells, are associated with the process together [145]. Thus, compared to *in vitro* models, this *murine* model is closer to the clinical scenario, reflecting the complicated interactions of numerous types of cells and tissues. Additionally, this *murine* model also reflects the effect of synovial fluid [79]. Because PAMPs, such as endotoxins, can activate TLRs, endotoxin-free CoCrMo materials were used in this investigation to eliminate the relative interfering factors.

4.2 TLRs 4 and 6

The CI group had a higher number of cells that showed positive staining with TLRs 4 and 6 antibodies than the PBS group in this investigation. Similarly, Bannon et al. [152] detected elevated TLR 4 expression in a murine model after nickel (Ni) stimulation. Samelko et al. [153] observed a strong TLR 4 based inflammatory response after CoCrMo/LPS+ or CoCrMo metal stimulation in a murine calvaria model. However, in

a study of contact allergy, Schmidt et al. [127, 128] indicated that Co^{2+} ions or Ni^{2+} ions (concentration 1.5 mM) could activate a pro-inflammatory response by directly binding to TLR 4 in humans but not in mice. These authors revealed that the non-conserved histidines 456 and 458 in human TLR 4 are critical components for activating inflammation by directly binding to Co^{2+} ions or Ni^{2+} ions. Nevertheless, murine TLR 4 does not contain these two non-conserved histidines mentioned above. Therefore, direct TLR 4 activation by Co^{2+} ions or Ni^{2+} ions was species-specific. As outlined above, the elevated expression levels of TLR 4 in the synovial layer of our murine model do not appear to be attributable to the direct effects of Co^{2+} ions or Ni^{2+} ions. Because the CoCrMo alloy used in this investigation also contains some other elements, e.g., molybdenum and chromium, the increased TLR 4 expression levels may be directly caused by other elements [76]. The effects of some other metal elements cannot be excluded in this study.

In addition, because metallic ions usually have complicated chemical and physical properties, the biological effects of metallic ions on the synovial layer do not appear to be limited to a single pathway. In addition to direct activation via ligand-receptor recognition, TLRs can also be indirectly activated by high concentrations of metallic ions [117]. Because metallic ions at high levels are usually toxic for normal cells. Briefly, metallic ions at high levels trigger the release of endogenous ligands of TLRs, e.g., some DAMPs delivered from injured or dying cells [154]. Upon the release of endogenous ligands, an indirect activation of TLRs can be observed. Likewise, the

metallic ion concentration used in this investigation is determined from the concentration detected in synovial fluid from patients scheduled for revision hip replacement, which might not be suitable for the knee joints of the murine model [137]. A concentration of metallic ions, which still has to be defined, probably leads to the release of DAMPs and subsequently results in the activation of TLR 4 and TLR 6. For patients with well-functioning prostheses in the clinical study, the metallic ion concentration in the synovial fluid is not usually even close to toxic levels [155]. A higher concentration of metal ions (toxic levels) in the synovial fluid is often observed in patients who need revision hip arthroplasty [137, 156]. Additionally, elevated TLR 4 and TLR 6 expressions were observed in periprosthetic tissues obtained from patients undergoing these revision surgeries [157, 158]. As described above, apart from the direct ligand-receptor recognition, the influence of metal ion concentration on TLR activation should not be neglected experimentally or clinically.

It was also found that the group injected with CoCrMo particles (CP) displayed a higher number of cells that had positive staining with TLR 4 and TLR 6 antibodies than the CI group. In the CP group, greenish corrosion particles were found in necrotic tissues, suggesting that metal particles were possible to be a reservoir of metal ions. A certain amount of metal ions was constantly released from metal particles within synovial tissues or cells through corrosion reactions. However, in the CI group, the primarily high amount of metal ions might unavoidably spread through lymphatic or blood vessels and finally be quenched throughout the whole body [159]. Metal ions that are

continuously released from metal particles appear to offer a sensible explanation for higher numbers of cells that showed positive staining with TLR 4 or TLR 6 antibodies in the CP group than those in the CI group.

CoCrMo implants commonly form an oxide film during manufacturing. The thickness of the oxide film is generally 1-4 nm, mainly containing Cr_2O_3 and CoO [160]. Due to the presence of the oxide film, the corrosion rate of the CoCrMo implants is effectively reduced. However, after the CoCrMo prosthesis is implanted, the oxide layer will be gradually destroyed because of wear and mechanical load [161]. Then, the unoxidized metal will be exposed to the physiological environment. Regardless, the corrosion process of CoCrMo implants in a physiological environment is relatively slow due to the existence of the oxide layer. In the present study, CoCrMo nanoparticles were directly injected into the murine knee joints. Unlike CoCrMo implants, these dispersed CoCrMo nanoparticles were phagocytized by macrophages in the synovial membrane and then exposed to intracellular reactive oxygen species [162]. After exposure, intracellular reactive oxygen species, such as superoxide and hypochlorous acid, underwent redox reactions with CoCrMo particles [92]. In this redox process, cells are injured, and some metal ions may be promptly released from metal particles. Necrotic tissues and green corrosion debris were found only seven days after the injection of the CoCrMo nanoparticles; this discovery might be associated to the redox reactions of CoCrMo nanoparticles outlined above.

4.3 TLR 1

Other than the electrochemical corrosion, the impacts of some distinct physical properties of CoCrMo particles, which are different from those of the CI group and the PBS group, should not be ignored. Several physical characteristics of wear particles, such as the volume, dose, shape, and size, exert a noticeable effect on periprosthetic biological reactions [86, 148, 163]. The thickness of cell membranes usually ranges from 4 nm to 10 nm [164]. Numerous studies have indicated that nanoparticles are able to damage and even perforate cell membranes. By means of hopping probe ion conductance microscopy, some researchers presented holes on the cellular surface damaged by nanoparticles [164]. In this study, the equivalent circular diameter of metallic nanoparticles was 61.25 ± 18.47 nm. It is highly possible for metallic nanoparticles to damage cell membranes directly under a particular situation in this study, especially when the knee joints of mice were in motion (with some pressure). When physical damage caused by nanoparticles occurs, injured cells activate distinct TLRs of adjacent immune cells and recruit more inflammatory cells, e.g., macrophages, by releasing DAMPs and pro-inflammatory mediators [165]. Along with phagocytizing wear particles, recruited macrophages express distinct TLRs that respond to the stimulation of adjacent danger signals [148, 165]. In this investigation, the CP group showed higher expression levels of TLR 1 than the CI group and the PBS group. However, no statistically obvious difference was found concerning the CI group and the PBS group. Thus, the elevated expression of TLR 1 in the CP group are possibly due to the unique properties of CoCrMo particles that differ from CoCrMo ions and

PBS, but more detailed investigations are required for further clarification.

4.4 TLRs 2 and 5

Because IL-6, TNF-α, and IL-1β, are the crucial pro-inflammatory cytokines present in tissues around implants and are even tightly associated with subsequent osteolysis, our institution used these three cytokines as markers of inflammation to assess the extent of pro-inflammatory reactions in the CP, CI, and PBS groups, respectively [24]. Based on the former results, the CP group showed higher IL-6, IL-1β, and TNF-α expressions than the control group. Interestingly, the results of three typical pro-inflammatory mediators were close to the results of TLR 2 and TLR 5 in the present study.

Greenfield et al. [124] observed that TLR $2^{-/-}$ murine macrophages expressed fewer TNF-α compared with normal macrophages after titanium debris challenge *in vitro*. Moreover, TLR 5 is regarded as a trigger of inflammatory responses. Kassem et al. [130] once showed that TLR 5 might have an important effect on the process of osteoclastogenesis and osteolysis caused by inflammatory reactions. These data strongly support the crucial roles of TLR 2 and TLR 5 in sterile inflammation to metal debris particles. TLR 2 and TLR 5 probably recognize the pro-inflammatory signals caused by wear debris through the indirect or direct way, then transduce these signals resulting in the secretion of several inflammatory mediators.

In previous studies, our research group found elevated TLR 2 expressions in the murine

knee joint synovial membrane after stimulation with UHMWPE wear particles [111], similar to our results from the CP group in this investigation. However, with regard to TLR 1 and TLR 4 expressions, the UHMWPE group did not have obvious difference compared to the control group in the previous study. One possible explanation for the difference between studies is the lack of an electrochemical corrosion process for UHMWPE particles relative to CoCrMo particles. Additionally, regarding the physical properties, UHMWPE particles had different sizes and shapes than the CoCrMo particles used in the present study. The extent of inflammatory reactions to wear particles is tightly correlated with particles' physical characteristics, such as shape and size [111]. Therefore, the physical properties of particles may also explain the discrepancy. Finally, both round macrophage-like cells and spindle-shaped fibroblast-like cells with positive reactions were counted in this study. However, the study examining UHMWPE particles only focused on round macrophage-like cells.

4.5 Limitations

This study has some limitations that must be considered. Undoubtedly, the murine model used in the present study adequately reflects pro-inflammatory responses in synovial-like tissues around implants. However, this *in vivo* model cannot be used to investigate subsequent osteolysis and aseptic implant loosening directly. With regard to animal models used for wear debris-mediated osteolysis, the air-pouch model and the calvaria model are representative models that have been widely used in several studies [166, 167]. These *in vivo* models of osteolysis also have some weaknesses because the

particle stimulation sites were not in the joints in these animal models, which are not close to the clinical scenario. Hence, the comprehensive development of an ideal animal model that potentially reflects the complicated mechanisms of sterile inflammation and subsequent aseptic loosening remains a challenge for future studies. This is also a research direction for our further studies.

A concentration gradient-related pretest involving CoCrMo particles and CoCrMo ions was not conducted in this study. For the gradient-related analysis, a larger number of mice is needed, which was not ethically acceptable in the current situation. The concentrations of CoCrMo particles and ions used here were based on previous experiments and some clinical studies [12, 111, 137]. The effects of different concentrations of wear debris on sterile inflammation will be studied in the future, aiming to determine the potential thresholds of dose for the sterile inflammation around implants.

Although we provide some new insights that clarify the effects of CoCrMo particles and CoCrMo ions on TLR expression in this study, the exact patterns of TLR activation relevant to CoCrMo debris still must be further elucidated. Although we observed significantly increased expression of distinct TLRs upon stimulation with CoCrMo particles or ions, we still cannot confirm whether the results were attributed to the direct or indirect effects of CoCrMo byproducts. The CoCrMo alloy composition is very complicated, and contains various metal elements, such as cobalt, chromium,

molybdenum, and nickel [168, 169]. The CoCrMo materials used in this study revealed the general impacts on TLR expression. The effects of single metal elements in CoCrMo alloys on TLR expression will also be investigated in the future, which will be very helpful to further understand the exact mechanisms of specific TLR activation.

5. Conclusions

The results clearly indicate that CoCrMo particles lead to an intense pro-inflammatory reaction and high expression of cell surface TLRs. In addition, green corrosion particles observed in this investigation suggest that CoCrMo particles may release a certain level of locally toxic ionic products. Significantly elevated expressions of TLR 4 and TLR 6 are found after CoCrMo ionic stimulation. The current results expose noticeable differences in TLR expression between animals injected with CoCrMo particles and CoCrMo ions *in vivo.*

6. Abbreviations

TLR	Toll-like receptor
CoCrMo	cobalt-chromium-molybdenum
CP	CoCrMo particles
CI	CoCrMo ions
PBS	phosphate-buffered saline
THR	total hip replacement
Pre	preoperative
Post	postoperative
ALTRs	adverse local tissue reactions
SLIM	synovial-like interface membrane
mo	macrophage
oc	osteoclast
CD 3	cluster of differentiation 3
MoM	metal-on-metal
ASTM	American Society for Testing and Materials
ISO	International Organization for Standardization
MoP	Metal-on-Polyethylene
µm	Micrometer
EDS	Energy-dispersive X-ray spectroscope
DNA	deoxyribonucleic acid

ROS	Reactive oxygen species
PRRs	Pattern Recognition Receptors
PAMPs	Pathogen-associated molecular patterns
DAMPs	Danger-associated molecular patterns
IL-1 β	Interleukin 1 β
IL-6	Interleukin 6
TNF-α	Tumor necrosis factor α
CD 281	cluster of differentiation 281
CD 282	cluster of differentiation 282
LPS	Lipopolysaccharide
RANKL	Receptor activator of nuclear factor kappa-B ligand
CD 286	cluster of differentiation 286
ECD	Equivalent Circular Diameter
AR	aspect ratio
R	Roundness
SEM	Scanning Electron Microscope
LAL	Limulus amebocyte lysate
g	gram
vol	volume
EDTA	Ethylenediaminetetraacetic acid
HIER	Heat induced epitope retrieval
HRP	Horseradish peroxidase

min	minute
ROI	region of interest
ANOVA	Analysis of variance
IHC	Immunohistochemistry
pH	power of hydrogen
PMMA	Poly (methyl methacrylate)
UHMWPE	ultra-high molecular weight polyethylene
PEEK	poly-ether-ether-ketone

7. Reference

1. Urban RM, Jacobs JJ, Tomlinson MJ, Gavrilovic J, Black J, Peoc'h M. Dissemination of wear particles to the liver, spleen, and abdominal lymph nodes of patients with hip or knee replacement. J Bone Joint Surg Am. 2000;82(4):457-76. Epub 2000/04/13. PubMed PMID: 10761937.

2. The-Swedish-Knee-Arthroplasty-Register. Annual Report 2010. Lund: 2010 10/7/2010. Report No.

3. Eriksson BI, Dahl OE, Rosencher N, Kurth AA, van Dijk CN, Frostick SP, et al. Dabigatran etexilate versus enoxaparin for prevention of venous thromboembolism after total hip replacement: a randomised, double-blind, non-inferiority trial. Lancet. 2007;370(9591):949-56. doi: 10.1016/S0140-6736(07)61445-7. PubMed PMID: 17869635.

4. Learmonth ID, Young C, Rorabeck C. The operation of the century: total hip replacement. Lancet. 2007;370(9597):1508-19. doi: 10.1016/S0140-6736(07)60457-7. PubMed PMID: 17964352.

5. Gallo J, Konttinen YT, Goodman S, Thyssen J, Gibon E, Pajarinen J, et al., editors. Aseptic Loosening of Total Hip Arthroplasty as a Result of Local Failure of Tissue Homeostasis2012.

6. Gallo J, Vaculova J, Goodman SB, Konttinen YT, Thyssen JP. Contributions of human tissue analysis to understanding the mechanisms of loosening and osteolysis in total hip replacement. Acta Biomater. 2014;10(6):2354-66. doi: 10.1016/j.actbio.2014.02.003. PubMed PMID: 24525037; PubMed Central PMCID: PMCPMC4389682.

7. Kurtz SM, Ong KL, Schmier J, Zhao K, Mowat F, Lau E. Primary and revision arthroplasty surgery caseloads in the United States from 1990 to 2004. J Arthroplasty. 2009;24(2):195-203. doi: 10.1016/j.arth.2007.11.015. PubMed PMID: 18534428.

8. Clohisy JC, Calvert G, Tull F, McDonald D, Maloney WJ. Reasons for revision hip surgery: a retrospective review. Clin Orthop Relat Res. 2004;(429):188-92. doi: 10.1097/01.blo.0000150126.73024.42. PubMed PMID: 15577486.

9. Apostu D, Lucaciu O, Berce C, Lucaciu D, Cosma D. Current methods of preventing aseptic loosening and improving osseointegration of titanium implants in cementless total hip arthroplasty: a review. J Int Med Res. 2018;46(6):2104-19. doi: 10.1177/0300060517732697. PubMed PMID: 29098919; PubMed Central PMCID: PMCPMC6023061.

10. Sundfeldt M, Carlsson LV, Johansson CB, Thomsen P, Gretzer C. Aseptic loosening, not only a question of wear: a review of different theories. Acta Orthop. 2006;77(2):177-97. doi: 10.1080/17453670610045902. PubMed PMID: 16752278.

11. Athanasou NA. The pathobiology and pathology of aseptic implant failure. Bone Joint Res. 2016;5(5):162-8. doi: 10.1302/2046-3758.55.BJR-2016-0086. PubMed PMID: 27146314; PubMed Central PMCID: PMCPMC4921050.

12. Paulus AC, Ebinger K, Cheng X, Hasselt S, Weber P, Kretzer JP, et al. Local Biological Reactions and Pseudotumor-Like Tissue Formation in relation to Metal Wear in a Murine In Vivo Model. Biomed Res Int. 2019;2019:3649838. doi: 10.1155/2019/3649838. PubMed PMID: 31781613; PubMed Central PMCID: PMCPMC6855077.

13. Goodman SB, Gibon E, Pajarinen J, Lin TH, Keeney M, Ren PG, et al. Novel biological strategies for treatment of wear particle-induced periprosthetic osteolysis of orthopaedic implants for joint replacement. J R Soc Interface. 2014;11(93):20130962. doi: 10.1098/rsif.2013.0962. PubMed PMID: 24478281; PubMed Central PMCID: PMCPMC3928932.

14. Lovelock TM, Broughton NS. Follow-up after arthroplasty of the hip and knee : are we over-servicing or under-caring? Bone Joint J. 2018;100-B(1):6-10. doi: 10.1302/0301-620X.100B1.BJJ-2017-0779.R1. PubMed PMID: 29305444.

15. Mumme T, Reinartz P, Alfer J, Muller-Rath R, Buell U, Wirtz DC. Diagnostic values of positron emission tomography versus triple-phase bone scan in hip arthroplasty loosening. Arch Orthop Trauma Surg. 2005;125(5):322-9. doi: 10.1007/s00402-005-0810-x. PubMed PMID: 15821896.

16. Mavrogenis AF, Dimitriou R, Parvizi J, Babis GC. Biology of implant osseointegration. J Musculoskelet Neuronal Interact. 2009;9(2):61-71. PubMed PMID: 19516081.

17. Mjoberg B. Theories of wear and loosening in hip prostheses. Wear-induced loosening vs loosening-induced wear--a review. Acta Orthop Scand. 1994;65(3):361-71. doi: 10.3109/17453679408995473. PubMed PMID: 8042497.

18. Rolvien T, Friesecke C, Butscheidt S, Gehrke T, Hahn M, Puschel K. A novel, multi-level approach to assess allograft incorporation in revision total hip arthroplasty. Sci Rep. 2020;10(1):15226. doi: 10.1038/s41598-020-72257-3. PubMed PMID: 32939007; PubMed Central PMCID: PMCPMC7494851.

19. Rajpura A, Kendoff D, Board TN. The current state of bearing surfaces in total hip replacement. Bone Joint J. 2014;96-B(2):147-56. doi: 10.1302/0301-620X.96B2.31920. PubMed PMID: 24493177.

20. Freeman MA, Plante-Bordeneuve P. Early migration and late aseptic failure of proximal femoral prostheses. J Bone Joint Surg Br. 1994;76(3):432-8. PubMed PMID: 8175848.

21. Derbyshire B, Prescott RJ, Porter ML. Notes on the use and interpretation of radiostereometric analysis. Acta Orthop. 2009;80(1):124-30. doi: 10.1080/17453670902807474. PubMed PMID: 19234894; PubMed Central PMCID: PMCPMC2823227.

22. Aspenberg P, Wagner P, Nilsson KG, Ranstam J. Fixed or loose? Dichotomy in RSA data for cemented cups. Acta Orthop. 2008;79(4):467-73. doi: 10.1080/17453670710015445. PubMed PMID: 18766478.

23. Willert HG, Semlitsch M. Reactions of the articular capsule to wear products of artificial joint prostheses. Journal of biomedical materials research. 1977;11(2):157-64. Epub 1977/03/01. doi: 10.1002/jbm.820110202. PubMed PMID: 140168.

24. Cheng X, Dirmeier SC, Hasselt S, Baur-Melnyk A, Kretzer JP, Bader R, et al. Biological Reactions to Metal Particles and Ions in the Synovial Layer of Mice. Materials (Basel). 2020;13(5). doi: 10.3390/ma13051044. PubMed PMID: 32110869; PubMed Central PMCID: PMCPMC7084385.

25. Jones MD, Buckle CL. How does aseptic loosening occur and how can we prevent it? Orthopaedics and Trauma. 2020;34(3):146-52.

26. Jacobs JJ, Hallab NJ, Urban RM, Wimmer MA. Wear particles. J Bone Joint Surg Am. 2006;88 Suppl 2:99-102. doi: 10.2106/JBJS.F.00102. PubMed PMID: 16595453.

27. Gallo J, Goodman SB, Konttinen YT, Wimmer MA, Holinka M. Osteolysis around total knee arthroplasty: a review of pathogenetic mechanisms. Acta Biomater. 2013;9(9):8046-58. doi: 10.1016/j.actbio.2013.05.005. PubMed PMID: 23669623.

28. Revell PA. The combined role of wear particles, macrophages and lymphocytes in the loosening of total joint prostheses. J R Soc Interface. 2008;5(28):1263-78. Epub 2008/07/24. doi: 10.1098/rsif.2008.0142. PubMed PMID: 18647740; PubMed Central PMCID: PMC2607446.

29. Gallo J, Kaminek P, Ticha V, Rihakova P, Ditmar R. Particle disease. A comprehensive theory of periprosthetic osteolysis: a review. Biomed Pap Med Fac Univ Palacky Olomouc Czech Repub. 2002;146(2):21-8. doi: 10.5507/bp.2002.004. PubMed PMID: 12572890.

30. Bitar D, Parvizi J. Biological response to prosthetic debris. World J Orthop. 2015;6(2):172-89. doi: 10.5312/wjo.v6.i2.172. PubMed PMID: 25793158; PubMed Central PMCID: PMCPMC4363800.

31. Dattani R. Femoral osteolysis following total hip replacement. Postgrad Med J. 2007;83(979):312-6. doi: 10.1136/pgmj.2006.053215. PubMed PMID: 17488859; PubMed Central PMCID: PMCPMC2600070.

32. Carbone A, Howie DW, McGee M, Field J, Pearcy M, Smith N, et al. Aging performance of a compliant layer bearing acetabular prosthesis in an ovine hip arthroplasty model. J Arthroplasty. 2006;21(6):899-906. doi: 10.1016/j.arth.2005.07.023. PubMed PMID: 16950047.

33. Mihalko WM, Haider H, Kurtz S, Marcolongo M, Urish K. New materials for hip and knee joint replacement: What's hip and what's in kneed? J Orthop Res. 2020;38(7):1436-44. doi: 10.1002/jor.24750. PubMed PMID: 32437026.

34. Cooper HJ, Urban RM, Wixson RL, Meneghini RM, Jacobs JJ. Adverse local tissue reaction arising from corrosion at the femoral neck-body junction in a dual-taper stem with a cobalt-chromium modular neck. J Bone Joint Surg Am. 2013;95(10):865-72. doi: 10.2106/JBJS.L.01042. PubMed PMID: 23677352; PubMed Central PMCID: PMCPMC3748981.

35. Gill HS, Grammatopoulos G, Adshead S, Tsialogiannis E, Tsiridis E. Molecular and immune toxicity of CoCr nanoparticles in MoM hip arthroplasty. Trends Mol Med. 2012;18(3):145-55. doi: 10.1016/j.molmed.2011.12.002. PubMed PMID: 22245020.

36. Eltit F, Wang Q, Wang R. Mechanisms of Adverse Local Tissue Reactions to Hip Implants. Front Bioeng Biotechnol. 2019;7:176. doi: 10.3389/fbioe.2019.00176. PubMed PMID: 31417898; PubMed Central PMCID: PMCPMC6683860.

37. Bates C, Marino V, Fazzalari NL, Bartold PM. Soft tissue attachment to titanium implants coated with growth factors. Clin Implant Dent Relat Res. 2013;15(1):53-63. doi: 10.1111/j.1708-8208.2010.00327.x. PubMed PMID: 21435158.

38. Krenn V, Perino G. Histological diagnosis of implant-associated pathologies. Histological Diagnosis of Implant-Associated Pathologies: Springer; 2017. p. 1-44.

39. Gallo J, Gibon E, Goodman S. Implants for joint replacement of the hip and knee. Materials for Bone Disorders: Elsevier; 2017. p. 119-96.

40. Abrahams JM, Kim YS, Callary SA, De Ieso C, Costi K, Howie DW, et al. The diagnostic performance of radiographic criteria to detect aseptic acetabular component loosening after revision total hip arthroplasty. Bone Joint J. 2017;99-B(4):458-64. doi: 10.1302/0301-620X.99B4.BJJ-2016-0804.R1. PubMed PMID: 28385934.

41. Perino G, Sunitsch S, Huber M, Ramirez D, Gallo J, Vaculova J, et al. Diagnostic guidelines for the histological particle algorithm in the periprosthetic neo-synovial tissue. BMC Clin Pathol. 2018;18:7. doi: 10.1186/s12907-018-0074-3. PubMed PMID: 30158837; PubMed Central PMCID: PMCPMC6109269.

42. Hu C, Ashok D, Nisbet DR, Gautam V. Bioinspired surface modification of orthopedic implants for bone tissue engineering. Biomaterials. 2019;219:119366. doi: 10.1016/j.biomaterials.2019.119366. PubMed PMID: 31374482.

43. Goldring S, Schiller A, Roelke M, Rourke C, O'neil D, Harris W. The synovial-like membrane at the bone-cement interface in loose total hip replacements and its proposed role in bone lysis. JBJS. 1983;65(5):575-84.

44. Morawietz L, Classen R, Schröder J, Dynybil C, Perka C, Skwara A, et al. Proposal for a histopathological consensus classification of the periprosthetic interface membrane. Journal of clinical pathology. 2006;59(6):591-7.

45. Yang F, Wu W, Cao L, Huang Y, Zhu Z, Tang T, et al. Pathways of macrophage apoptosis within the interface membrane in aseptic loosening of prostheses. Biomaterials. 2011;32(35):9159-67. doi: 10.1016/j.biomaterials.2011.08.039. PubMed PMID: 21872327.

46. Mescher AL. Macrophages and fibroblasts during inflammation and tissue repair in models of organ regeneration. Regeneration (Oxf). 2017;4(2):39-53. doi: 10.1002/reg2.77. PubMed PMID: 28616244; PubMed Central PMCID: PMCPMC5469729.

47. Abu-Amer Y, Darwech I, Clohisy JC. Aseptic loosening of total joint replacements: mechanisms underlying osteolysis and potential therapies. Arthritis Res Ther. 2007;9 Suppl 1:S6. doi: 10.1186/ar2170. PubMed PMID: 17634145; PubMed Central PMCID: PMCPMC1924521.

48. Esposito C, Maclean F, Campbell P, Walter WL, Walter WK, Bonar SF. Periprosthetic tissues from third generation alumina-on-alumina total hip arthroplasties. J Arthroplasty. 2013;28(5):860-6. doi: 10.1016/j.arth.2012.10.021. PubMed PMID: 23489720.

49. Gallo J, Goodman SB, Konttinen YT, Raska M. Particle disease: biologic mechanisms of periprosthetic osteolysis in total hip arthroplasty. Innate immunity. 2013;19(2):213-24. doi: 10.1177/1753425912451779. PubMed PMID: 22751380; PubMed Central PMCID: PMC3712274.

50. Whitehouse MR, Endo M, Zachara S, Nielsen TO, Greidanus NV, Masri BA, et al. Adverse local tissue reactions in metal-on-polyethylene total hip arthroplasty due to trunnion corrosion: the risk of misdiagnosis. Bone Joint J. 2015;97-B(8):1024-30. doi: 10.1302/0301-620X.97B8.34682. PubMed PMID: 26224816.

51. Granchi D, Savarino LM, Ciapetti G, Baldini N. Biological effects of metal degradation in hip arthroplasties. Crit Rev Toxicol. 2018;48(2):170-93. doi: 10.1080/10408444.2017.1392927. PubMed PMID: 29130357.

52. Ricciardi BF, Nocon AA, Jerabek SA, Wilner G, Kaplowitz E, Goldring SR, et al. Histopathological characterization of corrosion product associated adverse local tissue reaction in hip implants: a study of 285 cases. BMC Clin Pathol. 2016;16:3. doi: 10.1186/s12907-016-0025-9. PubMed PMID: 26924942; PubMed Central PMCID: PMCPMC4769839.

53. Langton DJ, Joyce TJ, Jameson SS, Lord J, Van Orsouw M, Holland JP, et al. Adverse reaction to metal debris following hip resurfacing: the influence of component type, orientation and volumetric wear. J Bone Joint Surg Br. 2011;93(2):164-71. doi: 10.1302/0301-620X.93B2.25099. PubMed PMID: 21282753.

54. Mahendra G, Pandit H, Kliskey K, Murray D, Gill HS, Athanasou N. Necrotic and inflammatory changes in metal-on-metal resurfacing hip arthroplasties. Acta Orthop. 2009;80(6):653-9. doi: 10.3109/17453670903473016. PubMed PMID: 19995315; PubMed Central PMCID: PMCPMC2823316.

55. Perino G, Ricciardi BF, Jerabek SA, Martignoni G, Wilner G, Maass D, et al. Implant based differences in adverse local tissue reaction in failed total hip arthroplasties: a morphological and immunohistochemical study. BMC Clin Pathol. 2014;14:39. doi: 10.1186/1472-6890-14-39. PubMed PMID: 25242891; PubMed Central PMCID: PMCPMC4169255.

56. Goodman SB. Wear particles, periprosthetic osteolysis and the immune system. Biomaterials. 2007;28(34):5044-8. Epub 2007/07/25. doi: 10.1016/j.biomaterials.2007.06.035. PubMed PMID: 17645943; PubMed Central PMCID: PMC2065897.

57. Wang Y, Dai S. Structural basis of metal hypersensitivity. Immunol Res. 2013;55(1-3):83-90. doi: 10.1007/s12026-012-8351-1. PubMed PMID: 22983897; PubMed Central PMCID: PMCPMC4040395.

58. Teo Wendy ZW, Schalock PC. Hypersensitivity Reactions to Implanted Metal Devices: Facts and Fictions. J Investig Allergol Clin Immunol. 2016;26(5):279-94. doi: 10.18176/jiaci.0095. PubMed PMID: 27763855.

59. Burkandt A, Katzer A, Thaler K, Von Baehr V, Friedrich RE, Ruther W, et al. Proliferation of the synovial lining cell layer in suggested metal hypersensitivity. In Vivo. 2011;25(4):679-86. PubMed PMID: 21709014.

60. Quigley L, Sprague S, Bhandari M. Pseudotumors following total hip and knee arthroplasty. Joint Evidence. 2010:1-33.

61. Iwamoto T, Ikari K, Momohara S. Pseudotumor from a metal-on-metal hip. J Rheumatol. 2011;38(10):2265. Epub 2011/10/04. doi: 10.3899/jrheum.110806. PubMed PMID: 21965694.

62. Kovochich M, Finley BL, Novick R, Monnot AD, Donovan E, Unice KM, et al. Understanding outcomes and toxicological aspects of second generation metal-on-metal hip implants: a state-of-the-art review. Crit Rev Toxicol. 2018;48(10):853-901. doi: 10.1080/10408444.2018.1563048. PubMed PMID: 30912993.

63. Merola M, Affatato S. Materials for Hip Prostheses: A Review of Wear and Loading Considerations. Materials (Basel). 2019;12(3). doi: 10.3390/ma12030495. PubMed PMID: 30764574; PubMed Central PMCID: PMCPMC6384837.

64. International ASfTaMA. ASTM F2003 - 02(2008) Standard Practice for Accelerated Aging of Ultra-High Molecular Weight Polyethylene after Gamma Irradiation in Air. 2008.

65. Toh WQ, Tan X, Bhowmik A, Liu E, Tor SB. Tribochemical Characterization and Tribocorrosive Behavior of CoCrMo Alloys: A Review. Materials (Basel). 2017;11(1). doi: 10.3390/ma11010030. PubMed PMID: 29278375; PubMed Central PMCID: PMCPMC5793528.

66. Bormann T, Mai PT, Gibmeier J, Sonntag R, Muller U, Kretzer JP. Corrosion Behavior of Surface-Treated Metallic Implant Materials. Materials (Basel). 2020;13(9). doi: 10.3390/ma13092011. PubMed PMID: 32344822; PubMed Central PMCID: PMCPMC7254368.

67. Buscher R, Tager G, Dudzinski W, Gleising B, Wimmer MA, Fischer A. Subsurface microstructure of metal-on-metal hip joints and its relationship to wear particle generation. J Biomed Mater Res B Appl Biomater. 2005;72(1):206-14. doi: 10.1002/jbm.b.30132. PubMed PMID: 15497166.

68. Pilliar RM. Metallic biomaterials. Biomedical materials: Springer; 2009. p. 41-81.

69. Gilbert JL, Sivan S, Liu Y, Kocagoz SB, Arnholt CM, Kurtz SM. Direct in vivo inflammatory cell-induced corrosion of CoCrMo alloy orthopedic implant surfaces. J Biomed Mater Res A. 2015;103(1):211-23. doi: 10.1002/jbm.a.35165. PubMed PMID: 24619511; PubMed Central PMCID: PMCPMC4162871.

70. Chen Y, Li Y, Kurosu S, Yamanaka K, Tang N, Chiba A. Effects of microstructures on the sliding behavior of hot-pressed CoCrMo alloys. Wear. 2014;319(1-2):200-10.

71. Oskouei RH, Barati MR, Farhoudi H, Taylor M, Solomon LB. A new finding on the in-vivo crevice corrosion damage in a CoCrMo hip implant. Materials Science and Engineering: C. 2017;79:390-8.

72. Narushima T, Ueda K. Co-Cr Alloys as Effective Metallic Biomaterials. Advances in Metallic Biomaterials: Springer; 2015. p. 157-78.

73. Asri R, Harun W, Samykano M, Lah N, Ghani S, Tarlochan F, et al. Corrosion and surface modification on biocompatible metals: A review. Materials Science and Engineering: C. 2017;77:1261-74.

74. Topolovec M, Cör A, Milošev I. Metal-on-metal vs. metal-on-polyethylene total hip arthroplasty tribological evaluation of retrieved components and periprosthetic tissue. Journal of the mechanical behavior of biomedical materials. 2014;34:243-52.

75. Kovochich M, Finley BL, Novick R, Monnot AD, Donovan E, Unice KM, et al. Understanding outcomes and toxicological aspects of second generation metal-on-metal hip implants: a state-of-the-art review. Critical reviews in toxicology. 2018;48(10):839-87.

76. Pourzal R, Catelas I, Theissmann R, Kaddick C, Fischer A. Characterization of Wear Particles Generated from CoCrMo Alloy under Sliding Wear Conditions. Wear. 2011;271(9-10):1658-66. doi: 10.1016/j.wear.2010.12.045. PubMed PMID: 21804652; PubMed Central PMCID: PMCPMC3144580.

77. Surgeons AAoO. Current concerns with metal-on-metal hip arthroplasty. 2015.

78. Rajpura A, Kendoff D, Board T. The current state of bearing surfaces in total hip replacement. The bone & joint journal. 2014;96(2):147-56.

79. Catelas I, Wimmer MA, Utzschneider S, editors. Polyethylene and metal wear particles: characteristics and biological effects. Seminars in immunopathology; 2011: Springer.

80. Barnes CL, DeBoer D, Corpe RS, Nambu S, Carroll M, Timmerman I. Wear performance of large-diameter differential-hardness hip bearings. The Journal of arthroplasty. 2008;23(6):56-60.

81. Nine MJ, Choudhury D, Hee AC, Mootanah R, Osman NAA. Wear debris characterization and corresponding biological response: artificial hip and knee joints. Materials. 2014;7(2):980-1016.

82. Sahasrabudhe H, Bose S, Bandyopadhyay A. Laser processed calcium phosphate reinforced CoCrMo for load-bearing applications: Processing and wear induced damage evaluation. Acta biomaterialia. 2018;66:118-28.

83. Madl AK, Liong M, Kovochich M, Finley BL, Paustenbach DJ, Oberdörster G. Toxicology of wear particles of cobalt-chromium alloy metal-on-metal hip implants Part I: Physicochemical properties in patient and simulator studies. Nanomedicine: nanotechnology, biology and medicine. 2015;11(5):1201-15.

84. Hussein MA, Mohammed AS, Al-Aqeeli N. Wear characteristics of metallic biomaterials: a review. Materials. 2015;8(5):2749-68.

85. Wahlström J, Lyu Y, Matjeka V, Söderberg A. A pin-on-disc tribometer study of disc brake contact pairs with respect to wear and airborne particle emissions. Wear. 2017;384:124-30.

86. Utzschneider S, Paulus A, Datz JC, Schroeder C, Sievers B, Wegener B, et al. Influence of design and bearing material on polyethylene wear particle generation in total knee replacement. Acta Biomater. 2009;5(7):2495-502. Epub 2009/04/21. doi: 10.1016/j.actbio.2009.03.016. PubMed PMID: 19375997.

87. Liao Y, Hoffman E, Wimmer M, Fischer A, Jacobs J, Marks L. CoCrMo metal-on-metal hip replacements. Physical Chemistry Chemical Physics. 2013;15(3):746-56.

88. Tipper J, Hatton A, Nevelos J, Ingham E, Doyle C, Streicher R, et al. Alumina–alumina artificial hip joints. Part II: characterisation of the wear debris from in vitro hip joint simulations. Biomaterials. 2002;23(16):3441-8.

89. Mordas G, Jasulaitienė V, Steponavičiūtė A, Gaspariūnas M, Petkevič R, Selskienė A, et al. Characterisation of CoCrMo powder for additive manufacturing. The International Journal of Advanced Manufacturing Technology. 2020;111(11):3083-93.

90. Hart AJ, Quinn PD, Sampson B, Sandison A, Atkinson KD, Skinner JA, et al. The chemical form of metallic debris in tissues surrounding metal-on-metal hips with unexplained failure. Acta biomaterialia. 2010;6(11):4439-46.

91. Mischler S, Munoz AI. Wear of CoCrMo alloys used in metal-on-metal hip joints: a tribocorrosion appraisal. Wear. 2013;297(1-2):1081-94.

92. Liu Y, Chen B. In vivo corrosion of CoCrMo alloy and biological responses: a review. Materials technology. 2018;33(2):127-34.

93. Gustafson HH, Holt-Casper D, Grainger DW, Ghandehari H. Nanoparticle Uptake: The Phagocyte Problem. Nano Today. 2015;10(4):487-510. doi: 10.1016/j.nantod.2015.06.006. PubMed PMID: 26640510; PubMed Central PMCID: PMCPMC4666556.

94. Anderson JM, Rodriguez A, Chang DT. Foreign body reaction to biomaterials. Semin Immunol. 2008;20(2):86-100. doi: 10.1016/j.smim.2007.11.004. PubMed PMID: 18162407; PubMed Central PMCID: PMCPMC2327202.

95. Silver I, Murrills R, Etherington D. Microelectrode studies on the acid microenvironment beneath adherent macrophages and osteoclasts. Experimental cell research. 1988;175(2):266-76.

96. Turk B, Turk V. Lysosomes as "suicide bags" in cell death: myth or reality? J Biol Chem. 2009;284(33):21783-7. doi: 10.1074/jbc.R109.023820. PubMed PMID: 19473965; PubMed Central PMCID: PMCPMC2755904.

97. Ishida Y, Nayak S, Mindell JA, Grabe M. A model of lysosomal pH regulation. J Gen Physiol. 2013;141(6):705-20. doi: 10.1085/jgp.201210930. PubMed PMID: 23712550; PubMed Central PMCID: PMCPMC3664703.

98. Gilbert JL, Kubacki GW. Oxidative stress, inflammation, and the corrosion of metallic biomaterials: Corrosion causes biology and biology causes corrosion. Oxidative Stress and Biomaterials: Elsevier; 2016. p. 59-88.

99. Liu Y, Gilbert JL. The effect of simulated inflammatory conditions and Fenton chemistry on the electrochemistry of CoCrMo alloy. Journal of Biomedical Materials Research Part B: Applied Biomaterials. 2018;106(1):209-20.

100. Prasad MNV. Trace elements as contaminants and nutrients: consequences in ecosystems and human health: John Wiley & Sons; 2008.

101. Andrews RE, Shah KM, Wilkinson JM, Gartland A. Effects of cobalt and chromium ions at clinically equivalent concentrations after metal-on-metal hip replacement on human osteoblasts and osteoclasts: implications for skeletal health. Bone. 2011;49(4):717-23.

102. Sauvé P, Mountney J, Khan T, De Beer J, Higgins B, Grover M. Metal ion levels after metal-on-metal Ring total hip replacement: a 30-year follow-up study. The Journal of bone and joint surgery British volume. 2007;89(5):586-90.

103. Urban RM, Jacobs JJ, Tomlinson MJ, Gavrilovic J, Black J, Peoc'h M. Dissemination of wear particles to the liver, spleen, and abdominal lymph nodes of patients with hip or knee replacement. JBJS. 2000;82(4):457.

104. Jacobs JJ, Skipor AK, Doorn PF, Campbell P, Schmalzried TP, Black J, et al. Cobalt and chromium concentrations in patients with metal on metal total hip replacements. Clinical Orthopaedics and Related Research®. 1996;329:S256-S63.

105. Thierse H-J, Gamerdinger K, Junkes C, Guerreiro N, Weltzien HU. T cell receptor (TCR) interaction with haptens: metal ions as non-classical haptens. Toxicology. 2005;209(2):101-7.

106. Büdinger L, Hertl M, Büdinger L. Immunologic mechanisms in hypersensitivity reactions to metal ions: an overview. Allergy. 2000;55(2):108-15.

107. Martin SF, Jakob T. From innate to adaptive immune responses in contact hypersensitivity. Current opinion in allergy and clinical immunology. 2008;8(4):289-93.

108. Takeuchi O, Akira S. Pattern recognition receptors and inflammation. Cell. 2010;140(6):805-20.

109. Athanasou N. The pathobiology and pathology of aseptic implant failure. Bone & joint research. 2016;5(5):162-8.

110. Nich C, Goodman SB. Role of macrophages in the biological reaction to wear debris from joint replacements. Journal of long-term effects of medical implants. 2014;24(4).

111. Paulus AC, Frenzel J, Ficklscherer A, Rossbach BP, Melcher C, Jansson V, et al. Polyethylene wear particles induce TLR 2 upregulation in the synovial layer of mice. J Mater Sci Mater Med. 2014;25(2):507-13. doi: 10.1007/s10856-013-5095-y. PubMed PMID: 24249629.

112. Grandjean-Laquerriere A, Tabary O, Jacquot J, Richard D, Frayssinet P, Guenounou M, et al. Involvement of toll-like receptor 4 in the inflammatory reaction induced by hydroxyapatite particles. Biomaterials. 2007;28(3):400-4. doi: 10.1016/j.biomaterials.2006.09.015. PubMed PMID: 17010424.

113. Pajarinen J, Mackiewicz Z, Pollanen R, Takagi M, Epstein NJ, Ma T, et al. Titanium particles modulate expression of Toll-like receptor proteins. J Biomed Mater Res A. 2010;92(4):1528-37. doi: 10.1002/jbm.a.32495. PubMed PMID: 19425045.

114. Bitar D, Parvizi J. Biological response to prosthetic debris. World journal of orthopedics. 2015;6(2):172.

115. McKiel LA, Woodhouse KA, Fitzpatrick LE. The role of Toll-like receptor signaling in the macrophage response to implanted materials. MRS Communications. 2020;10(1):55-68.

116. Hopkins P, Sriskandan S. Mammalian Toll-like receptors: to immunity and beyond. Clinical & Experimental Immunology. 2005;140(3):395-407.

117. Takagi M, Takakubo Y, Pajarinen J, Naganuma Y, Oki H, Maruyama M, et al. Danger of frustrated sensors: Role of Toll-like receptors and NOD-like receptors in aseptic and septic inflammations around total hip replacements. J Orthop Translat. 2017;10:68-85. doi: 10.1016/j.jot.2017.05.004. PubMed PMID: 29130033; PubMed Central PMCID: PMCPMC5676564.

118. Elfeil WM, Algammal AM, Abouelmaatti RR, Gerdouh A, Abdeldaim M. Molecular characterization and analysis of TLR-1 in rabbit tissues. Central-European journal of immunology. 2016;41(3):236.

119. Le Rossignol S, Ketheesan N, Haleagrahara N. Redox-sensitive transcription factors play a significant role in the development of rheumatoid arthritis. International reviews of immunology. 2018;37(3):129-43.

120. Farhat K, Riekenberg S, Heine H, Debarry J, Lang R, Mages J, et al. Heterodimerization of TLR2 with TLR1 or TLR6 expands the ligand spectrum but does not lead to differential signaling. J Leukoc Biol. 2008;83(3):692-701. doi: 10.1189/jlb.0807586. PubMed PMID: 18056480.

121. Pajarinen J, Mackiewicz Z, Pöllänen R, Takagi M, Epstein NJ, Ma T, et al. Titanium particles modulate expression of Toll-like receptor proteins. Journal of Biomedical Materials Research Part A: An Official Journal of The Society for Biomaterials, The Japanese Society for Biomaterials, and The Australian Society for Biomaterials and the Korean Society for Biomaterials. 2010;92(4):1528-37.

122. Rock FL, Hardiman G, Timans JC, Kastelein RA, Bazan JF. A family of human receptors structurally related to Drosophila Toll. Proc Natl Acad Sci U S A. 1998;95(2):588-93. doi: 10.1073/pnas.95.2.588. PubMed PMID: 9435236; PubMed Central PMCID: PMCPMC18464.

123. de Oliviera Nascimento L, Massari P, Wetzler L. The Role of TLR2 in Infection and Immunity. Frontiers in Immunology. 2012;3(79). doi: 10.3389/fimmu.2012.00079.

124. Greenfield EM, Beidelschies MA, Tatro JM, Goldberg VM, Hise AG. Bacterial pathogen-associated molecular patterns stimulate biological activity of orthopaedic wear particles by activating cognate Toll-like receptors. J Biol Chem. 2010;285(42):32378-84. doi: 10.1074/jbc.M110.136895. PubMed PMID: 20729214; PubMed Central PMCID: PMC2952239.

125. Qureshi ST, Lariviere L, Leveque G, Clermont S, Moore KJ, Gros P, et al. Endotoxin-tolerant mice have mutations in Toll-like receptor 4 (Tlr4). J Exp Med. 1999;189(4):615-25. doi: 10.1084/jem.189.4.615. PubMed PMID: 9989976; PubMed Central PMCID: PMCPMC2192941.

126. Poltorak A, He X, Smirnova I, Liu M-Y, Van Huffel C, Du X, et al. Defective LPS signaling in C3H/HeJ and C57BL/10ScCr mice: mutations in Tlr4 gene. Science. 1998;282(5396):2085-8.

127. Raghavan B, Martin SF, Esser PR, Goebeler M, Schmidt M. Metal allergens nickel and cobalt facilitate TLR4 homodimerization independently of MD2. EMBO Rep. 2012;13(12):1109-15. doi: 10.1038/embor.2012.155. PubMed PMID: 23059983; PubMed Central PMCID: PMCPMC3512400.

128. Schmidt M, Raghavan B, Muller V, Vogl T, Fejer G, Tchaptchet S, et al. Crucial role for human Toll-like receptor 4 in the development of contact allergy to nickel. Nat Immunol. 2010;11(9):814-9. doi: 10.1038/ni.1919. PubMed PMID: 20711192.

129. Gomariz R, Arranz A, Juarranz Y, Gutierrez-Canas I, Garcia-Gomez M, Leceta J, et al. Regulation of TLR expression, a new perspective for the role of VIP in immunity. Peptides. 2007;28(9):1825-32.

130. Kassem A, Henning P, Kindlund B, Lindholm C, Lerner UH. TLR5, a novel mediator of innate immunity-induced osteoclastogenesis and bone loss. FASEB J. 2015;29(11):4449-60. doi: 10.1096/fj.15-272559. PubMed PMID: 26207027.

131. Takeuchi O, Kawai T, Sanjo H, Copeland NG, Gilbert DJ, Jenkins NA, et al. TLR6: A novel member of an expanding toll-like receptor family. Gene. 1999;231(1-2):59-65. doi: 10.1016/s0378-1119(99)00098-0. PubMed PMID: 10231569.

132. Shmuel-Galia L, Klug Y, Porat Z, Charni M, Zarmi B, Shai Y. Intramembrane attenuation of the TLR4-TLR6 dimer impairs receptor assembly and reduces microglia-mediated neurodegeneration. J Biol Chem. 2017;292(32):13415-27. doi: 10.1074/jbc.M117.784983. PubMed PMID: 28655763; PubMed Central PMCID: PMCPMC5555200.

133. Stewart CR, Stuart LM, Wilkinson K, van Gils JM, Deng J, Halle A, et al. CD36 ligands promote sterile inflammation through assembly of a Toll-like receptor 4 and 6 heterodimer. Nat Immunol. 2010;11(2):155-61. doi: 10.1038/ni.1836. PubMed PMID: 20037584; PubMed Central PMCID: PMCPMC2809046.

134. Roy R, Singh SK, Das M, Tripathi A, Dwivedi PD. Toll-like receptor 6 mediated inflammatory and functional responses of zinc oxide nanoparticles primed macrophages. Immunology.

2014;142(3):453-64. doi: 10.1111/imm.12276. PubMed PMID: 24593842; PubMed Central PMCID: PMCPMC4080961.

135. Liao Y, Pourzal R, Stemmer P, Wimmer M, Jacobs J, Fischer A, et al. New insights into hard phases of CoCrMo metal-on-metal hip replacements. Journal of the mechanical behavior of biomedical materials. 2012;12:39-49.

136. Catelas I, Wimmer MA, Utzschneider S. Polyethylene and metal wear particles: characteristics and biological effects. Seminars in immunopathology. 2011;33(3):257-71. Epub 2011/01/27. doi: 10.1007/s00281-011-0242-3. PubMed PMID: 21267569.

137. De Smet K, De Haan R, Calistri A, Campbell PA, Ebramzadeh E, Pattyn C, et al. Metal ion measurement as a diagnostic tool to identify problems with metal-on-metal hip resurfacing. J Bone Joint Surg Am. 2008;90 Suppl 4:202-8. doi: 10.2106/JBJS.H.00672. PubMed PMID: 18984732.

138. Bogen SA, Vani K, Sompuram SR. Molecular mechanisms of antigen retrieval: antigen retrieval reverses steric interference caused by formalin-induced cross-links. Biotech Histochem. 2009;84(5):207-15. doi: 10.3109/10520290903039078. PubMed PMID: 19886757; PubMed Central PMCID: PMCPMC4676902.

139. Hira VV, de Jong AL, Ferro K, Khurshed M, Molenaar RJ, Van Noorden CJ. Comparison of different methodologies and cryostat versus paraffin sections for chromogenic immunohistochemistry. Acta histochemica. 2019;121(2):125-34.

140. Goodman SB, Gallo J. Periprosthetic Osteolysis: Mechanisms, Prevention and Treatment. J Clin Med. 2019;8(12). doi: 10.3390/jcm8122091. PubMed PMID: 31805704; PubMed Central PMCID: PMCPMC6947309.

141. Krenn V, Perino G, Krenn VT, Wienert S, Saberi D, Hugle T, et al. [Histopathological diagnostic work-up of joint endoprosthesis-associated pathologies]. Hautarzt. 2016;67(5):365-72. doi: 10.1007/s00105-016-3778-2. PubMed PMID: 26987961.

142. Zysk SP, Gebhard H, Plitz W, Buchhorn GH, Sprecher CM, Jansson V, et al. Influence of orthopedic particulate biomaterials on inflammation and synovial microcirculation in the murine knee joint. J Biomed Mater Res B Appl Biomater. 2004;71(1):108-15. Epub 2004/09/16. doi: 10.1002/jbm.b.30075. PubMed PMID: 15368234.

143. Zysk SP, Gebhard HH, Kalteis T, Schmitt-Sody M, Jansson V, Messmer K, et al. Particles of all sizes provoke inflammatory responses in vivo. Clin Orthop Relat Res. 2005;(433):258-64. Epub 2005/04/05. PubMed PMID: 15805966.

144. Utzschneider S, Becker F, Grupp TM, Sievers B, Paulus A, Gottschalk O, et al. Inflammatory response against different carbon fiber-reinforced PEEK wear particles compared with UHMWPE in vivo. Acta Biomater. 2010;6(11):4296-304. Epub 2010/06/24. doi: 10.1016/j.actbio.2010.06.002. PubMed PMID: 20570640.

145. Utzschneider S, Lorber V, Dedic M, Paulus AC, Schroder C, Gottschalk O, et al. Biological activity and migration of wear particles in the knee joint: an in vivo comparison of six different polyethylene materials. J Mater Sci Mater Med. 2014;25(6):1599-612. Epub 2014/02/25. doi: 10.1007/s10856-014-5176-6. PubMed PMID: 24562818.

146. Ramani V, Madhusoodhanan R, Kosanke S, Awasthi S. A TLR4-interacting SPA4 peptide inhibits LPS-induced lung inflammation. Innate immunity. 2013;19(6):596-610. doi: 10.1177/1753425912474851. PubMed PMID: 23475791.

147. Kimball A, Krueger J, Sullivan T, Arbeit R. IMO-3100, an antagonist of Toll-like receptor (TLR) 7 and TLR9, demonstrates clinical activity in psoriasis patients with 4 weeks of treatment in a phase 2a trial International Investigative Dermatology Meeting. Edinburgh, Scotland. Journal of Investigative Dermatology. 2013:S26.

148. Paulus AC, Hasselt S, Jansson V, Giurea A, Neuhaus H, Grupp TM, et al. Histopathological Analysis of PEEK Wear Particle Effects on the Synovial Tissue of Patients. Biomed Res Int. 2016;2016:2198914. Epub 2016/10/22. doi: 10.1155/2016/2198914. PubMed PMID: 27766256; PubMed Central PMCID: PMCPMC5059511.

149. Green TR, Fisher J, Matthews JB, Stone MH, Ingham E. Effect of size and dose on bone resorption activity of macrophages by in vitro clinically relevant ultra high molecular weight polyethylene particles. Journal of Biomedical Materials Research: An Official Journal of The Society for Biomaterials, The Japanese Society for Biomaterials, and The Australian Society for Biomaterials and the Korean Society for Biomaterials. 2000;53(5):490-7.

150. Ren W, Yang S-Y, Fang H-W, Hsu S, Wooley PH. Distinct gene expression of receptor activator of nuclear factor-κB and rank ligand in the inflammatory response to variant morphologies of UHMWPE particles. Biomaterials. 2003;24(26):4819-26.

151. Jonitz-Heincke A, Tillmann J, Klinder A, Krueger S, Kretzer JP, Hol PJ, et al. The Impact of Metal Ion Exposure on the Cellular Behavior of Human Osteoblasts and PBMCs: In Vitro Analyses of Osteolytic Processes. Materials (Basel). 2017;10(7). Epub 2017/08/05. doi: 10.3390/ma10070734. PubMed PMID: 28773099; PubMed Central PMCID: PMCPMC5551777.

152. Bannon DI, Bao W, Turner SD, McCain WC, Dennis W, Wolfinger R, et al. Gene expression in mouse muscle over time after nickel pellet implantation. Metallomics. 2020;12(4):528-38. doi: 10.1039/c9mt00289h. PubMed PMID: 32065191.

153. Samelko L, Landgraeber S, McAllister K, Jacobs J, Hallab NJ. TLR4 (not TLR2) dominate cognate TLR activity associated with CoCrMo implant particles. J Orthop Res. 2017;35(5):1007-17. Epub 2016/07/15. doi: 10.1002/jor.23368. PubMed PMID: 27416075.

154. Herrero-Beaumont G, Perez-Baos S, Sanchez-Pernaute O, Roman-Blas JA, Lamuedra A, Largo R. Targeting chronic innate inflammatory pathways, the main road to prevention of osteoarthritis progression. Biochem Pharmacol. 2019;165:24-32. doi: 10.1016/j.bcp.2019.02.030. PubMed PMID: 30825432.

155. Back DL, Young D, Shimmin A. How do serum cobalt and chromium levels change after metal-on-metal hip resurfacing? Clinical Orthopaedics and Related Research®. 2005;438:177-81.

156. Jacobs JJ, Skipor AK, Patterson LM, Hallab NJ, Paprosky WG, Black J, et al. Metal release in patients who have had a primary total hip arthroplasty. A prospective, controlled, longitudinal study. JBJS. 1998;80(10):1447-58.

157. Li, Wang H, Li Z, Wang C, Xiao F, Gao Y, et al. The inhibition of RANKL expression in fibroblasts attenuate CoCr particles induced aseptic prosthesis loosening via the MyD88-independent TLR signaling pathway. Biochem Biophys Res Commun. 2018;503(2):1115-22. doi: 10.1016/j.bbrc.2018.06.128. PubMed PMID: 29940143.

158. Takagi M, Tamaki Y, Hasegawa H, Takakubo Y, Konttinen L, Tiainen VM, et al. Toll-like receptors in the interface membrane around loosening total hip replacement implants. J Biomed Mater Res A. 2007;81(4):1017-26. doi: 10.1002/jbm.a.31235. PubMed PMID: 17415764.

159. Sansone V, Pagani D, Melato M. The effects on bone cells of metal ions released from orthopaedic implants. A review. Clin Cases Miner Bone Metab. 2013;10(1):34-40. doi: 10.11138/ccmbm/2013.10.1.034. PubMed PMID: 23858309; PubMed Central PMCID: PMCPMC3710008.

160. Eliaz N. Corrosion of Metallic Biomaterials: A Review. Materials (Basel). 2019;12(3). doi: 10.3390/ma12030407. PubMed PMID: 30696087; PubMed Central PMCID: PMCPMC6384782.

161. Liao Y, Hoffman E, Wimmer M, Fischer A, Jacobs J, Marks L. CoCrMo metal-on-metal hip replacements. Phys Chem Chem Phys. 2013;15(3):746-56. doi: 10.1039/c2cp42968c. PubMed PMID: 23196425; PubMed Central PMCID: PMCPMC3530782.

162. Abdal Dayem A, Hossain MK, Lee SB, Kim K, Saha SK, Yang GM, et al. The Role of Reactive Oxygen Species (ROS) in the Biological Activities of Metallic Nanoparticles. Int J Mol Sci. 2017;18(1). doi: 10.3390/ijms18010120. PubMed PMID: 28075405; PubMed Central PMCID: PMCPMC5297754.

163. Schroder C, Reinders J, Zietz C, Utzschneider S, Bader R, Kretzer JP. Characterization of polyethylene wear particle: The impact of methodology. Acta Biomater. 2013;9(12):9485-91. doi: 10.1016/j.actbio.2013.07.039. PubMed PMID: 23933100.

164. Sukhanova A, Bozrova S, Sokolov P, Berestovoy M, Karaulov A, Nabiev I. Dependence of Nanoparticle Toxicity on Their Physical and Chemical Properties. Nanoscale Res Lett. 2018;13(1):44. doi: 10.1186/s11671-018-2457-x. PubMed PMID: 29417375; PubMed Central PMCID: PMCPMC5803171.

165. Zhang X, Mosser DM. Macrophage activation by endogenous danger signals. J Pathol. 2008;214(2):161-78. doi: 10.1002/path.2284. PubMed PMID: 18161744; PubMed Central PMCID: PMCPMC2724989.

166. Gelb H, Ralph Schumacher H, Cuckler J, Baker DG. In vivo inflammatory response to polymethylmethacrylate particulate debris: effect of size, morphology, and surface area. Journal of orthopaedic research. 1994;12(1):83-92.

167. Merkel KD, Erdmann JM, McHugh KP, Abu-Amer Y, Ross FP, Teitelbaum SL. Tumor necrosis factor-α mediates orthopedic implant osteolysis. The American journal of pathology. 1999;154(1):203-10.

168. 17853. IOfSI. Wear of implant particles - polymer and metal weat particles - isolation, characterization and quantification. Geneva: International Organization for Standardization. 2008.

169. Cheng X, Jansson V, Kretzer JP, Bader R, Utzschneider S, Paulus AC. The expression levels of Toll-like receptors after metallic particle and ion exposition in the synovium of a murine model. Journal of Clinical Medicine. 2021; 10(16):3489.

8. Appendix

Appendix 1. Descriptive statistics for TLR 1, 2, 4, 5, and 6

Proteins	TLR 1			TLR 2		
Groups	CP	CI	PBS	CP	CI	PBS
Minimum	78.30	44.20	7.250	41.50	21.00	2.200
25% Percentile	110.1	57.33	23.43	75.30	26.75	8.688
Median	192.5	73.75	37.50	99.20	34.58	14.38
75% Percentile	224.9	108.0	83.33	128.0	44.83	25.45
Maximum	232.2	114.0	100.8	150.5	89.25	53.40
Range	153.9	69.80	93.50	109.0	68.25	51.20
Mean	175.3	78.90	49.18	98.24	40.70	18.10
Std. Deviation	59.80	26.15	33.16	33.80	20.54	14.74
Std. Error of Mean	19.93	7.885	11.05	10.69	5.929	4.662
Proteins	TLR 4			TLR 5		
Groups	CP	CI	PBS	CP	CI	PBS
Minimum	67.25	28.50	7.250	37.40	18.50	11.25
25% Percentile	80.01	44.69	17.50	59.80	35.33	14.30
Median	96.53	68.65	29.70	133.4	44.63	21.00
75% Percentile	135.3	84.15	35.88	152.3	63.53	23.60
Maximum	157.2	125.3	72.50	171.0	84.50	66.50
Range	89.95	96.80	65.25	133.6	66.00	55.25
Mean	104.7	67.69	30.91	115.8	48.32	24.42
Std. Deviation	32.23	28.35	18.42	48.28	18.28	17.62
Std. Error of Mean	10.19	8.185	6.139	14.56	5.277	6.229
Proteins	TLR 6					
Groups	CP	CI	PBS			
Minimum	74.30	45.00	15.80			
25% Percentile	120.6	58.01	26.65			
Median	142.6	74.42	33.30			
75% Percentile	189.2	91.78	45.25			
Maximum	205.0	99.40	72.75			
Range	130.7	54.40	56.95			
Mean	147.2	74.81	37.07			
Std. Deviation	42.12	18.45	16.48			
Std. Error of Mean	13.32	5.326	5.493			

CP, CoCrMo particles. CI, CoCrMo ions. PBS, phosphate-buffered saline. TLRs, Toll-like receptors

9. Statement

This research was funded by the German Research Foundation (DFG; funding number: UT 444 119/3-1, BA 3347/12-1, and KR 3755/5-1). As a part of the DFG-funded cooperative project, production and analysis of CoCrMo particles and ions were finished by our cooperative team at University of Heidelberg. For *in vivo* trials, the intra-articular injection of mice was performed by my colleague, Dr. med. Kathrin Ebinger. There is no conflict of interest.

All experimental procedures relevant to mice were performed according to the rules and regulations of the Animal Protection Laboratory Animal Regulations (2013) and European Directive 2010/63/EU Act and approved by the government of Upper Bavaria, Germany (protocol number: 55.2-1-54-2532-82.12).

For Figure 9, 10, 11, 12, and 13, we have published them in Journal of Clinical Medicine (MDPI publisher) [169]. Cheng, X.; Jansson, V.; Kretzer, J.P.; Bader, R.; Utzschneider, S.; Paulus, A.C. The Expression Levels of Toll-Like Receptors after Metallic Particle and Ion Exposition in the Synovium of a Murine Model. J. Clin. Med. 2021, 10, 3489. https://doi.org/10.3390/jcm10163489. There is no potential conflict of interest according to the statement of MDPI publisher:For all articles published in MDPI journals, copyright is retained by the authors. Articles are licensed under an open access Creative Commons CC BY 4.0 license, meaning that anyone may download and read the paper for free. In addition, the article may be reused and quoted provided that the

original published version is cited. These conditions allow for maximum use and exposure of the work, while ensuring that the authors receive proper credit.

Acknowledgments

In October 2017, I came to Munich to achieve the degree Dr. rer. biol. hum. The study process was challenging but hopeful, and it was a truly unforgettable experience in my life. During my time in Munich, many kind-hearted people gave me a great amount of professional advice and encouragement, without which this thesis would not have been completed. Thus, I would like to express my heartfelt thanks to those who have helped me over these years:

I would like to thank my Head of the Department, Professor Dr. med. Boris Holzapfel, and Professor Dipl.-Ing. Dr. med. Volkmar Jansson, former director of the Department of Orthopedics, Physical Medicine and Rehabilitation, University Hospital of Munich (LMU), Germany, for allowing me to do my research project in the Laboratory of Biomechanics & Experimental Orthopedics.

I would also like t**o** express my deepest thanks to Prof. Dr. med. Sandra Utzschneider, for inviting me to do my doctoral study in Munich. I am very grateful for her moral support, which introduced me to and provided me with an understanding of the field of biological reactions to wear debris released from implants.

Subsequently, I would like to convey my sincere appreciation to my supervisor, P. D. Dr. med. Alexander C. Paulus, for his continuous guidance and support. His meticulous and enlightening teachings were of great help to my research work, especially the

drafting and submission of papers. His solid theoretical foundation and positive mentality inspired my strong interest and love for scientific exploration. As an orthopedic surgeon, he helped one of my friends treat femoral head necrosis, which made me more passionate and interested in modern medicine. In a foreign land, I always have warm feelings and feel relaxed after communicating with him. Thanks again!

I also sincerely would like to thank Dr. Roland M. Klar, the Regenerative Medicine Leader of the Laboratory I did my studies in, who has always provided his reliable help. With the guidance of Dr. Roland Klar, I received systemic training of scientific research in the laboratory, which has built core fundamental principles critical for my future work. Thank you for assisting me in solving various difficulties during the entire experiment, in conjunction with your rigorous attitude towards scientific research, which profoundly influenced me.

I would also like to thank the medical technicians, Ms. Bärbel Schmitt and Ms. Sandra Haßelt, for their technical support and patiently teaching me several techniques. Without their help, I would have never been able to finish my projects. They taught me how to do cell culture, histology, immunohistochemistry, etc., which enriched my knowledge and became the driving force for me to push forward. Additionally, I would like to thank all the other laboratory members, especially Dr. Matthias Woiczinski and Mr. Michael Kraxenberger, for their selfless help during my stay in our laboratory.

I would also like to thank my Chinese friends, Xiansheng Liu, Lingxi Ye, Tao He, Yijiang Huang, Fanxiao Liu, Fei Xiong, and Heng Liu, for their companionship and encouragement. In a foreign country, they treated me as one of their family members and provided much enthusiastic help for my daily life. I hope to see you again and recall this wonderful time together!

My doctoral study was funded by China Scholarship Council (CSC). The project was funded by German Research Foundation. Because of their financial support, I was able to study at this prestigious university founded by Ludwig-Maximillian. Thanks very much. Additionally, I would also like to thank Prof. Dr. med. Jan Philippe Kretzer, Prof. Dr. med. Rainer Bader and Dr. med. Kathrin Ebinger for their support in this project and valuable advice in the revision of the published manuscripts.

Finally, I would like to thank deeply my family for their continuous moral and emotional support in my life. My parents, my sister, and my girlfriend, I feel extremely fortunate to own you. Thank you for teaching me how to love unconditionally, and most of all, thank you for loving me unconditionally no matter what.

List of Figures

List of Tables

List of Appendixes